Electronic Supplementary Material (ESI) for Materials Horizons.
This journal is © The Royal Society of Chemistry 2019

Electronic Supplementary Information

Hybrid 'clusterbombs' as multifunctional nanoplatforms potentiate brain tumor immunotherapy

Qi Shen,[ab1] Jun Yang,[a1] Ruiyuan Liu,[a] Linying Liu,[a] Jinchao Zhang,[b] Shigang Shen*[b] and Xin Zhang*[a]

Experimental Section

Materials and Reagents. 2-Aminoethanethiol hydrochloride, 2,2'-dithiodipyridine, methacrylic anhydride, N-hydroxysuccinimide, 3-mercaptopropionic acid, N-(3-dimethylaminopropyl)-N'-ethylcarbodiimide hydrochloride, 4,4'-azobis(4-cyanovaleric acid), 4-cyano-4-(dodecylsulfanylthiocarbonyl) sulfanylpentanoic acid, 4-cyano-4-(phenylcarbonothioylthio)pentanoic acid, 4,4'-azobis(4-cyanovaleric acid), 2-(dimethylamino)ethyl methacrylate, tert-butyl bromoacetate, 2-(dimethylamino)ethyl acrylate, 4-aminophenyl α-D-mannopyranoside, 6-maleimidohexanoic acid N-hydroxysuccinimide ester, hexamethylene diamine and cystamine dihydrochloridewere obtained from J&K Scientific Ltd., Co (Shanghai, China). Triethylamine, trifluoroacetic acid (TFA), 2,2'-dicyano-2,2'-azopropane (AIBN) was purchased from Aladdin Industrial Corporation (Shanghai, China). PEPvIII (LEEKKGNYVVTDHC) was synthesized by GL Biochem Ltd (Shanghai, China). Cell Titer 96® AQueous One Solution Cell Proliferation Assay was purchased from Promega (Beijing, China). Dulbecco's Modified Eagle Medium (DMEM), L-glutamine, penicillin (10,000 U/mL), streptomycin (10 mg/mL), trypsin-EDTA and fetal bovine serum (FBS), and Lysotracker Red DND-99 were purchased from Invitrogen (Carlsbad, CA, USA). Paraformaldehyde and 4',6-diamidino-2-phenylindole dihydrochloride (DAPI) were obtained from Solarbio Science & Technology Ltd, Co (Beijing, China). Phosphate-buffered saline (PBS, pH=7.4) and micro BCA protein assay kit were purchased from Beyotime Institute of Biotechnology (Nanjing, China). The dialysis bags (MWCO 3500) were purchased from Spectrum

Laboratories Inc (NJ, USA). All antibodies used for flow cytometry analysis and ELISA Kit were purchased from eBioscience (CA, USA), including flow cytometry cell staining buffer, Foxp3/transcription factor staining buffer set kit, 1×RBC lysis buffer, anti-rat CD4 FITC, anti-rat CD8a APC, anti-rat/mouse Foxp3 PE, anti-rat IFN-γ PerCP-Cyanine5.5. All the reagents were used as received without further purification. Other reagents were acquired from Sigma-Aldrich. High-purity water (Milli-Q Integral) with a conductivity of 18 MΩ cm^{-1} was used for the preparation of all aqueous solutions.

Cell lines and animals. $F98_{npEGFRvIII}$ rat glioblastoma cell lines were kindly provided by Prof. Fang Wang (Peking University, China). Cells were cultured in high glucose DMEM supplemented with 10% fetal bovine serum and 0.2 mg/mL G-418 at 37°C with 5% CO_2.

Female F344 rat (4-6 weeks) were purchased from Charles River Laboratories China. The animals were maintained under specific pathogen-free conditions. All animal studies were done in accordance with the guidelines evaluated and approved by the ethics committee of Tsing Hua University (Beijing, China).

Synthesis of ZnO nanoparticles. ZnO nanoparticles (ZnO NPs) were prepared by using the method as follow. Briefly, zinc acetate (203 mg, 2.0 mmol) and NaOH (52 mg, 2.5 mmol) were dissolved in hot ethanol (20 mL) under vigorous stirring at 70°C in two separate flasks. The solution was then cooled down in ice bath. Then NaOH solution was rapidly injected into the other flask containing dissolved zinc acetate. The mixture was stirred for 1 h for particles growth, and then the mixture solution was

precipitated using hexane as non-solvent. The resulting ZnO NPs showed green emission under UV lamp excitation.

Synthesis of sulfhydryl modified ZnO NPs. Precipitated ZnO NPs (100 mg) was dispersed in dimethyl sulfoxide (DMSO, 15 mL) while sonication. 3-Mercaptopropionic acid (1.07 mL) was then added to the solution. The reaction mixture was stirred at room temperature for 2 h. The precipitation of sulfhydryl modified ZnO NPs was isolated by centrifugation, and then dispersed in DMSO.

Synthesis and purification of PtCB polymers. Poly(t-butyloxycarbonylcarboxybetaine) (PtCB) was synthesized by the reversible addition-fragmentation chain transfer (RAFT) polymerization. The synthesis procedure with 2-tert-butoxy-N-(2-(methacryloyloxy)ethyl)-N,N-dimethyl-2 oxoethanaminium (CB-tBu) was described as follow. Briefly, 2-(dimethylamino)ethyl methacrylate (DMAEMA, 5.36 mL) and tert-butyl bromoacetate (tBu-BA, 6.49 mL) were dissolved in acetonitrile (20 mL) under nitrogen at room temperature for 30 min, and then stirred at 50°C for 1 day. The product (CB-tBu) was precipitated with ether and the monomer was immediately stored in desiccator at -20°C. ^{1}H NMR (600 MHz, $(CD_3)_2SO$, δ). δ=5.7-6.5 (2H, -COOC$\boldsymbol{H}_2$CH$_3$), δ=4.0-5.0 (4H, -CH$_3$C$\boldsymbol{H}_2$-, -COOC$\boldsymbol{H}_2$-), δ=3.9-4.0 (2H, -C$\boldsymbol{H}_2$NCH$_3$CH$_3$), δ=3.30 (6H, -NC$\boldsymbol{H}_3$CH$_3$), δ=1.8-2.0 (3H, -C$\boldsymbol{H}_3$), δ=1.2-1.4 (9H, -COO(C$\boldsymbol{H}_3$)$_3$).

The RAFT polymerization of PCB was conducted in anhydrous dimethyl sulfoxide using obtained CB-tBu (300 mg), 4-cyano-4-(phenylcarbonothioylthio) pentanoic acid (CPTP, 10.2 mg), and 4,4'-azobis(4-cyanovaleric acid) (ACVA, 2.0 mg). The system

was degassed by three freeze-pump-thaw cycles and recharged with nitrogen. The reaction mixture was stirred for 24 h at 65°C in a sealed environment. The resulting liquid was dialyzed overnight against deionized water using a Cellu SepH1-membrane (MWCO 3500) and then lyophilized to obtain the final product PtCB. ^{1}H NMR (600 MHz, D_2O, δ). δ=7.5-8.0 (5H, -C(C***H***)$_5$-), δ=4.2-4.6 (4H, -COOC***H***$_2$-,-C***H***$_2$N-), δ=3.8-4.2 (4H, -COOCH$_2$C***H***$_2$, -N(CH$_3$)$_2$C***H***$_2$-), δ=3.2-3.5 (6H, -NC***H***$_3$C***H***$_3$), δ=2.8-3.0 (2H, -C***H***$_2$COOH), δ=1.8-2.0 (3H, -COOCC***H***$_3$-), δ=1.3-1.5 (9H, -COOC(C***H***$_3$)$_3$), δ=0.88-1.2 (3H, -CNCC***H***$_3$).

Synthesis and purification of PDM-PDA polymers. 2-Aminoethanethiol hydrochloride (1.14 g, 0.01 mol) and 2,2'-dithiodipyridine (6.6 g, 0.03 mol) were dissolved in methanol (10 mL) at room temperature overnight. The resulting solution was precipitated with ether and then dissolved in methanol and precipitated repeatedly until acquired the white product (DTA). ^{1}H-NMR (600 MHz, (CD$_3$)$_2$SO, δ). δ=8.5-8.6 (1H, -NC***H***-), δ=8.3-8.5 (2H, -N***H***$_2$), δ=7.8-7.9 (1H, -NCHC***H***-), δ=7.7-7.8 (1H, -C***H***CHCH-), δ=7.3-7.5 (1H, -CC***H***-), δ=3.0-3.2 (4H, -C***H***$_2$C***H***$_2$NH$_2$).

The monomer DTA (4 g, 0.017 mol), methacrylic anhydride (2.8 mL, 0.085 mol) and anhydrous triethylamine (12.5 mL, 0.018 mol) were added in a clean round flask with anhydrous dichloromethane. The reaction mixture was stirred overnight at room temperature in the anhydrous environment. After the end of the reaction, the crude product was purified by flash chromatography using ethyl acetate and hexane as eluent and adsorbent respectively to afford the product of PDM. ^{1}H-NMR (600 MHz, (CD$_3$)$_2$SO, δ). δ=7.0-8.5 (4H, -N(C***H***)$_4$), δ=5.0-6.0 (6H, -C(C***H***$_3$)$_2$-), δ=4.2-4.4 (1H, -

CON***H***-), δ=3.5-3.7 (2H, -NHC$\boldsymbol{H}_2$-), δ=2.8-3.0 (2H, -$CH_2C\boldsymbol{H}_2$S-), δ=1.3-1.5 (3H, -C$\boldsymbol{H}_3$).

2-(Dimethylamino)ethyl acrylate (DA, 2.68 mL, 17.1 mmol), 4-cyano-4-(dodecylsulfanylthiocarbonyl) sulfanylpentanoic acid (CDSA, 79.3 mg, 0.19 mmol) and AIBN (6.45 mg, 0.03 mmol) were dissolved in 1,4-dioxane (2 mL), and then added into a clean and dry Schleck flask. The system was degassed by three freeze-pump-thaw cycles and recharged with nitrogen. The mixture solution was stirred at 60°C for 24 h. Then PDM (500 mg, 1.9 mmol) and AIBN (6.45 mg, 0.03 mmol) dissolved in 1,4-dioxane (3 mL) was added into the mixture and stirred for another 24 h. The solution was dialyzed against deionized water using a Cellu SepH1-membrane (MWCO 3500). The final product poly(N-(2-(2-pyridyldithio)) ethyl methyacrylamide)-b-poly(2-(dimethylamino) ethyl acrylate) (PDM-PDA) was obtained after the liquid lyophilized. ^{1}H-NMR (600 MHz, $(CD_3)_2SO$, δ). δ=8.0-8.4 (1H, -CON***H***-), δ=7.2-7.8 (5H, -C(C***H***)$_5$-), δ=4.0-4.2 (2H, -COOC$\boldsymbol{H}_2$-), δ=3.7-3.9 (2H, -CONHC$\boldsymbol{H}_2$-), δ=3.2-3.4 (4H, -C$\boldsymbol{H}_2$N$(CH_3)_2$, $CH_3(CH_2)_8C\boldsymbol{H}_2$-), δ=2.7-3.0 (8H, -$CONHCH_2C\boldsymbol{H}_2$-, -N(C$\boldsymbol{H}_3)_2$), δ=2.4-2.7 (2H,-$CH_3CC\boldsymbol{H}_2CH$-), δ=2.0-2.3 (3H, -$CH_2C\boldsymbol{H}$CCN-, -C$\boldsymbol{H}_2$COOH), δ=1.3-1.7 (3H, -CC$\boldsymbol{H}_3$), δ=1.1-1.2 (3H, -CC$\boldsymbol{H}_3$), δ=0.88-1.1 (19H, C$\boldsymbol{H}_3(C\boldsymbol{H}_2)_8$-).

Synthesis of GSH-responsiveness polymers (PCB-S-S-PDM-PDA, PSDP) and non-responsive polymers (PCB-PDM-PDA, PCDP). PtCB polymer (500 mg, 0.06 mmol), N-hydroxysuccinimide (NHS, 8.45 mg, 0.073 mmol) and N-(3-dimethylaminopropyl)-N'-ethylcarbodiimide hydrochloride (EDC, 14.07 mg, 0.073 mmol) were dissolved in 10 mL anhydrous DMSO at 25°C with gentle stirring for 30 min, and then added

cystamine dihydrochloride (68.9 mg, 0.3 mmol) with stirring for 24 h. PDM-PDA (944.2 mg, 0.06 mmol) was added and allowed to stir for 48 h. The impurities and unreacted molecules were removed by sequentially dialyzing in a Cellu SepH1-membrane (MWCO 7000) with deionized water and freeze-dried to obtain the product (PtCB-S-S-PDM-PDA). The obtained product was dissolved in DMSO, and then added 2 mL trifluoroacetic Acid (TFA) to remove blocking group. The solution was precipitated with ether and dispersed in DMF, then dialyzed by a Cellu SepH1-membrane (MWCO 7000) with deionized water to get PCB-S-S-PDM-PDA (PSDP). The control polymer PCB-C-PDM-PDA (PCDP) was synthesized with the similar route of PSDP, with cystamine dihydrochloride changing to hexamethylene diamine.

PSDP (500 mg) was then dissolved in DMSO (5 mL), and then hydrazine hydrate (100 μL) was added to the solution and allowed to stir at room temperature. 4-Aminophenyl α-D-mannopyranoside (Mannose, 16.6 mg, 0.06 mmol) and N-succinimidy 1-6-maleimidolexanoate (NHS-Linker-Mal, 18.9 mg, 0.06 mmol) were added in solution and stirred for 24 h at 25°C. The resulting liquid was dialyzed overnight against deionized water using a Cellu SepH1-membrane (MWCO 7000) and then lyophilized to obtain the final product Man-PCB-S-S-PDM-PDA (MPSDP). ^{1}H-NMR (600 MHz, $(CD_3)_2SO$, δ). δ=8.4-8.6 (3H, -$CH_2CH_2CON\boldsymbol{H}$-, -$SSCH_2CH_2N\boldsymbol{H}CO$-, -$CHCON\boldsymbol{H}$-), δ=7.7-7.1 (9H, -$CN(C\boldsymbol{H})_4$, -$C(C\boldsymbol{H})_4N\boldsymbol{H}$-), δ=4.0-5.0 (4H, -$COOC\boldsymbol{H}_2$-, -$N(CH_3)_2C\boldsymbol{H}_2$-), δ=3.1-3.7 (16H, -$COOCH_2C\boldsymbol{H}_2N(CH_3)_2$, -$C\boldsymbol{H}_2N(CH_3)_2$-, -$N(C\boldsymbol{H}_3)_2CH_2COO$-, -$CONHC\boldsymbol{H}_2CH_2SSCH_2C\boldsymbol{H}_2NHCO$-, -$NHC\boldsymbol{H}_2CH_2$-), δ=2.7-3.0 (1H, -C**H**COO-), δ=2.0-2.3 (18H, -$CONHCH_2C\boldsymbol{H}_2SSC\boldsymbol{H}_2CH_2NHCO$-, -$CHC\boldsymbol{H}_2C$-, -

$COOCH_2CH_2N(C\boldsymbol{H}_3)_2$, -$NHCOC\boldsymbol{H}_2CH_2C$-, -$CH_2C\boldsymbol{H}_2CONH$-, -$C\boldsymbol{H}_2(CH_2)_9CH_3$), δ=0.88-2.0 (41H, -$NHCO(C\boldsymbol{H}_2)_5$-, -$COOCC\boldsymbol{H}_3$, -$NHCOCC\boldsymbol{H}_3$-, -$CC\boldsymbol{H}_2CH_2CONH$-, -$NHCOCH_2C\boldsymbol{H}_2$-, -$(C\boldsymbol{H}_2)_9C\boldsymbol{H}_3$). The control copolymer Man-PCB-C-PDM-PDA (MPCDP) was also synthesized with the similar route of MPSDP.

Preparation and characterization of nanoparticles. To prepare reduction-responsive PSDP-ZnO/Ag nanoparticles, PSDP polymer (PCB-S-S-PDM-PDA) was dissolved in DMSO to obtain 10 mg/mL of polymer solution. Then, the prepared ZnO NPs was modified with thiol groups. 1 mg of thiol modified ZnO NPs and 2 mg of Ag were mixed in DMSO at room temperature for 2 h, then 20 mg of PSDP was added overnight. The obtained PSDP-ZnO/Ag was dialyzed with a dialysis membrane (MWCO 3500) in distilled water. The PSDP-ZnO/Ag was prepared with various formations at room temperature. The PCDP-ZnO/Ag was prepared with the similar method as PSDP-ZnO/Ag.

The mean particle diameters of the nanoparticles were evaluated by dynamic light scattering (DLS) and the surface charge were detected by the zeta potential using a Malvern Zetasizer nano ZS apparatus (Malvern Instruments, Malvern, United Kingdom). The morphology of nanoparticles was measured by using transmission electron microscopy (JEM-2100 electron microscope). The determination of disulfide bond in ZnO/Ag was used by Spectrophotometry.

The encapsulation efficiency of nanovaccines were determined as described as follow. To assess the Ag loading capacity (LC) of nanovaccines were ultra-centrifuged at 10,000×g for 20 min, and the amount of unbound Ag in supernatant was determined

using BCA Protein Assay Kit (Solarbio). The loading capacity calculated using the following equation (1):

LC = (total protein - unbound protein)/total dry weight of nanovaccine × 100% (1)

To test the serum stability, NPs with a concentration of 1mg/mL were incubated in PBS containing 10% FBS at room temperature. At each point in time, the size change of the PSDP-ZnO/Ag complexes were measured by using DLS.

In vitro release profile of Ag. To determine the redox-responsiveness of different nanoparticles, nanoparticles were incubated in PBS buffer with or without 10 mM GSH at 37°C. The nanoparticle sizes were observed at different time points by using TEM.

The released of antigen from nanovaccines were analyzed by dialysis method. Briefly, NPs were dialyzed in 2.0 mL PBS (PH=7.4) and were incubated in 50 mL PBS containing 0 or 10 mM GSH with gently shaking at 37°C. At predetermined time intervals, 1 mL aliquots of the medium were taken out and the same volume of fresh solution was supplemented. The released concentration of Ag in the incubated medium was detected by using fluorescence spectrum. The accumulative release of Ag was expressed as a percentage of the released Ag as a function of time.

Integrity of Ag. The PEPvIII antigen integrity was examined by Tricine-SDS-PAGE gel electrophoresis. Accordingly, 2 mg of nanoparticles were dispersed in 1 mL of 9% (w/v) sucrose solution. After 7 d, 14 d and 21 d of incubation, nanoparticles were collected by centrifugation, re-dissolved in 1 M GSH solution. Following overnight incubation at room temperature, centrifugation, supernatant was used for BCA protein

assay kit according to the manufacturer's instructions for 96-microwell plate. Supernatant was concentrated by using an Amicon 10 K membrane cenrifugal filter unit (Millipore). Moreover, 0.04 mg of antigen (corresponding to the amount of antigen encapsulated in nanoparticles) was used as control.

Cytotoxicity and cellular uptake of nanoparticles. *In vitro* cytotoxicity of nanoparticles were assessed by CellTiter 96® AQueous One Solution Cell Proliferation Assay. Cells were plated onto a 96-well culture plate at a density of 1×10^6 cells per well in 100 μL culture medium and allowed to attach overnight. Then, the culture medium was removed and replaced with 100 μL fresh culture medium containing 10-100 μg/mL of PSDP-ZnO/Ag for indicated time (24 h and 48 h) at 37°C with 5% CO_2. After 24 h or 48 h incubation, 20 μL test fluid was added to each well and incubated at 37°C in 5% CO_2 for 2 h. The absorbance was measured at 490 nm using a plate reader. The percentage of cell viability was determined by cells treated with different formulations to the untreated control cells.

For flow cytometry analysis, Immature BMDCs were treated with FITC-Ag or PSDP-ZnO/FITC-Ag in various lengths of time at 37°C. And then, the cells washed with cold PBS and incubated first with CD16/CD32 Fc block (at 4°C for 10 min, eBioscience, San Diego, CA) and then labeled with fluorescent antibody CD11c for 30 min at 4°C. The collected cells were then assessed with BD Calibur flow cytometry to test the fluorescence intensity of Ag.

The intracellular localization of Ag in DCs was determined by using confocal laser scanning microscopy (CLSM). In Brief, 2×10^5 DC2.4 cells were seeded in 35 mm

Petridishes for 24 h, and the medium was replaced with RPMI1640 containing 10% FBS, which including Ag, PSDP-Ag, PSDP-ZnO/Ag, PCDP-ZnO/Ag, MPCDP-ZnO/Ag and MPSDP-ZnO/Ag. The concentration of Ag was 40 μg/mL and the cells were then incubated for 2 h, 6 h and 48 h at 37°C, respectively. Subsequently, the cells were washed three times with PBS followed by labled with Lysotracker Red DND-99 (Invitrogen, CA, USA) for 30 min to visualize late endosomes and lysosomes. The cells were washed three times with PBS and fixed with fresh 4% paraformaldehyde for 10 min at room temperature. The nucleus were stained with DAPI for 10 min. Red fluorescence of Lysotracker Red, blue fluorescence of DAPI and green fluorescence of FITC were observed using a Zeiss LSM780 CLSM (Zeiss Co., Germany).

Tumor-associated dendritic cells (TADCs) culture and stimulation. To prepare tumor-conditioned medium, 5×10^6 $F98_{npEGFRvIII}$ rat glioblastoma cells were cultured in 100-mm Petri dish with 10 mL of DMEM with 10% FBS for 2 d, and supernatants ($F98_{npEGFRvIII}$-CM) were harvested and stored at -80°C until use. To acquire TADCs, rat bone marrow cells were cultured in DC culture medium (20 ng/mL GM-CSF and 10 ng/mL IL-4) supplemented with 20% $F98_{npEGFRvIII}$-CM (v/v) at 37°C for 6 d. On day 6, TADCs were re-suspended in fresh culture medium and stimulated with different formulations for another 48 h. At the end of the experiment, the cells were harvested and labeled with anti-rat CD11c combined with fluorescent antibody CD40, CD86, MHC I and MHC II on ice for 30 min. The expressions of CD40, CD86, MHC I or MHC II on TADCs cells were determined by using a BD Calibur flow cytometry. The

production of cytokines in supernatants was measured by using ELISA kits according to manufacturer's instruction.

Animal immunization and tumor treatment. The F98 rat glioma cell line derived from CD-Fischer 344 rats treated with N-ethyl-N-nitrosourea and transfected with Geneticin (G418) at a concentration of 100 μg/mL. F344 (CDF) rat were stereotactically implanted with 10^6 $F98_{npEGFRvIII}$ cells in 10 μL serum-free medium, and the cells were injected over 10 to 15 seconds through a central hole in a plastic screw into the right caudate nucleus. More than 95% of rat could recover from the surgery, and the incidence of glioma was almost 100%. Rats were observed daily and weighed thrice a week following tumor implantation to monitor their clinical status. Rats were randomly divided into 7 groups (n=10) and housed in a colony room at 22 ± 2°C and 45 ± 10% humidity under a 12:12 h light/dark cycle. On day 7, 17, 24 after glioma cell implantation, rats were injected with different cancer vaccines.

In vivo cytotoxic T lymphocyte (CTL) assay and tumor-specific-T-lymphocyte activation. Female F344 rats and tumor-bearing rats were immunized with different formulations. Total splenocytes were isolated from rats 7 days after last immunization. The red blood cells were removed by using red blood cells lysis buffer (eBioscience). And the lymphocytes were re-stimulated with 100 μg/mL of Ag in the presence of IL-2 (20 U/mL) for 24 h to acquire CTL effectors. The effectors and target cells ($F98_{npEGFRvIII}$) were cultured in 96-well plates at various effector/target (E:T) ratios for 6 h. Tumor-specific lysis was quantified by using CellTiter 96® AQueous One Solution Cell Proliferation Assay Kit according to manufacturer's instruction. For vaccine-

induced T cells response, splenocytes were harvested and acquired cells were stained with fluorescence-labeled antibodies according to the standard protocols. The cells were re-suspended in staining buffer and incubated with fluorescence antibodies against CD8, CD4, CD44 and CD62L. Then cells were mixed with 100 μL Foxp3 Fixation/permeabilization buffer (eBioscience), followed by 1×permeabilization buffer (eBioscience) was added. Finally, $CD4^+$, $CD8^+$, regulatory T cells (Treg) and memory T cells ($CD44^{Hi}CD62L^{Hi}$) were detected by using a BD Calicur flow cytometry.

Tumor-specific interferon gamma (IFN-γ) production. Tumor-bearing F344 rats were immunized with different formulations and sacrificed 7 d later. Spleen were harvested from each rat and processed into single cell suspensions. Tumor-specific IFN-γ production was measured by BD TM ELISPOT assay system according to the manufacturer's instructions. Briefly, cells with different vaccines were seeded into 96-well plates that were pre-coated with capture antibody and incubated in RPMI1640 media at 37°C. After 24 h, cells were removed and washed with PBS for 5 times. The production of IFN-γ was detected by adding detection antibody. The results were observed by using BD TM ELISPOT substrate set and enumerated manually after imaging.

Immunofluorescent staining assay. To investigate tumor infiltrating $CD8^+$ T cells, $CD4^+$ T cells and Treg cells in brain tumor section, brain tumors were removed from rat, paraffin embedding, and then cut into 8 μm-thick paraffin sections. The slides of paraffin sections of tumor tissues were permeabilized and fixed, and blocked with 1%

BSA at room temperature for 1 h, followed by incubation with anti-rat antibody against CD8, CD4, Foxp3 at room temperature for 2 h, respectively.

Statistical Analysis. All data were expressed as mean ± SD unless otherwise indicated. Statistical significance was analyzed by using one-way ANOVA. Statistical differences in behavioral data were determined by using two-way repeated measures ANOVA.

Table S1 The abbreviation of nanoparticles prepared in the experiments.

Full name	**Abbreviation**
(ZnO+PCB-S-S-PDM-PDA)	**PSDP-ZnO**
(Ag+PCB-S-S-PDM-PDA)	**PSDP-Ag**
(ZnO+Ag+PCB-S-S-PDM-PDA)	**PSDP-ZnO/Ag**
(ZnO+Ag+PCB-C-PDM-PDA)	**PCDP-ZnO/Ag**
(ZnO+Ag+Man-PCB-C-PDM-PDA)	**MPCDP-ZnO/Ag**
(ZnO+Ag+Man-PCB-S-S-PDM-PDA)	**MPSDP-ZnO/Ag**

Supplementary Figures

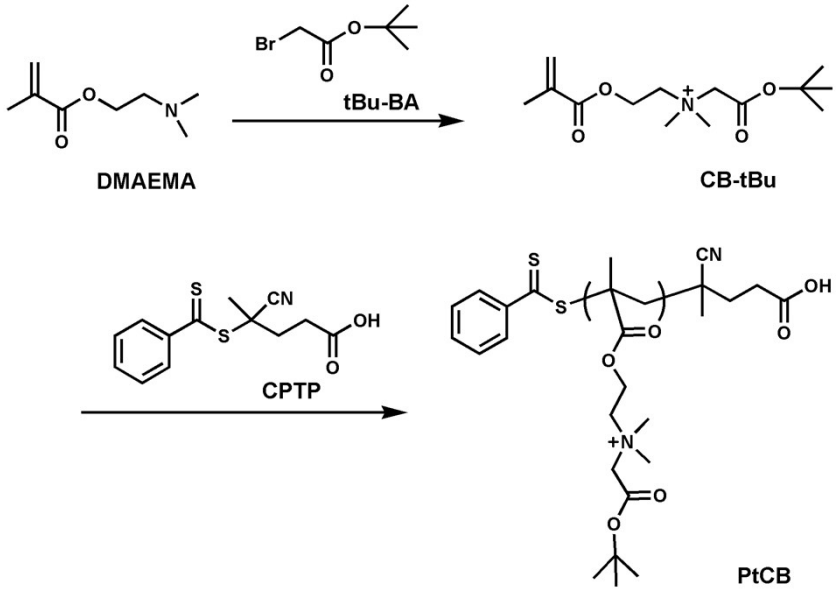

Fig. S1 The synthetic routes of poly (t-butyloxycarbonyl carboxybetaine) polymers (PtCB).

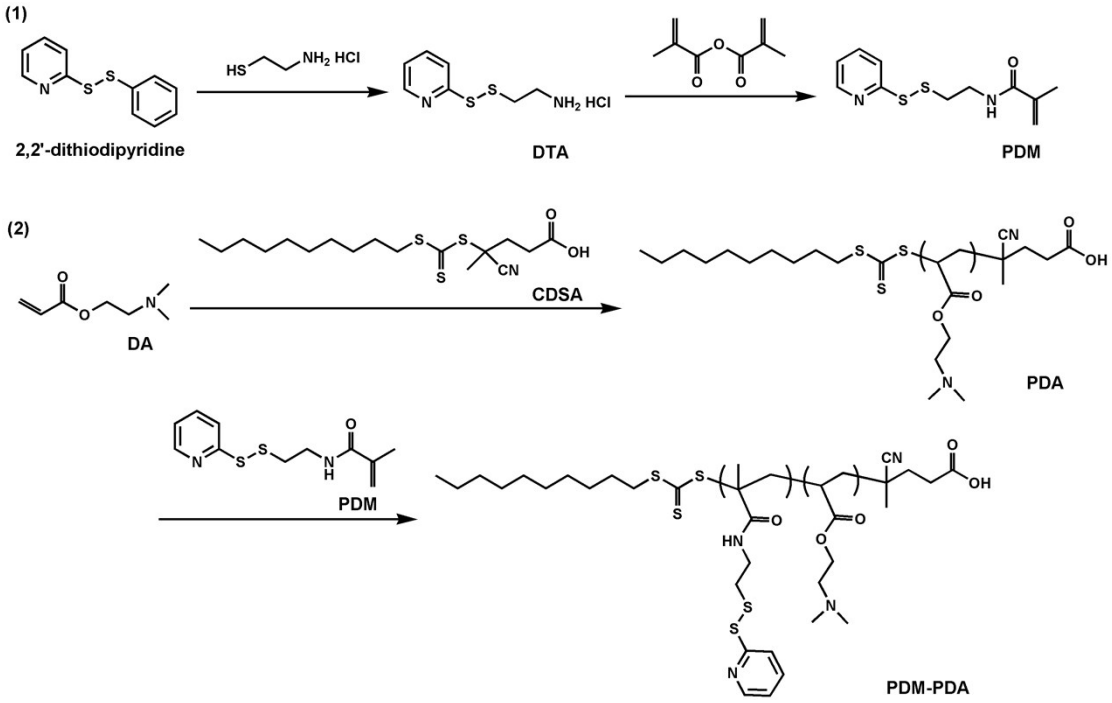

Fig. S2 The synthetic routes of (1) poly(N-(2-(2-pyridyldithio)) ethyl methyacrylamide) (PDM) and (2) poly(N-(2-(2-pyridyldithio)) ethyl methyacrylamide)-b-poly(2-(dimethylamino) ethyl acrylate) polymers (PDM-PDA).

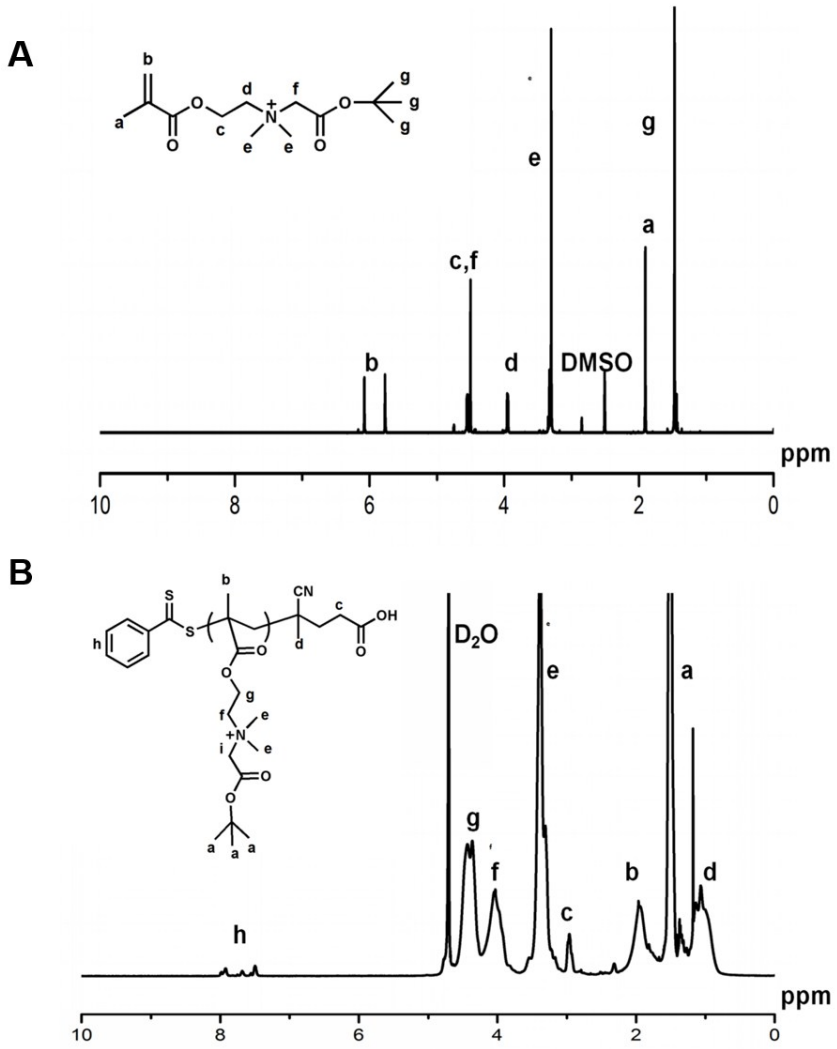

Fig. S3 ^{1}H NMR spectra of CB-tBu (A) and PtCB (B).

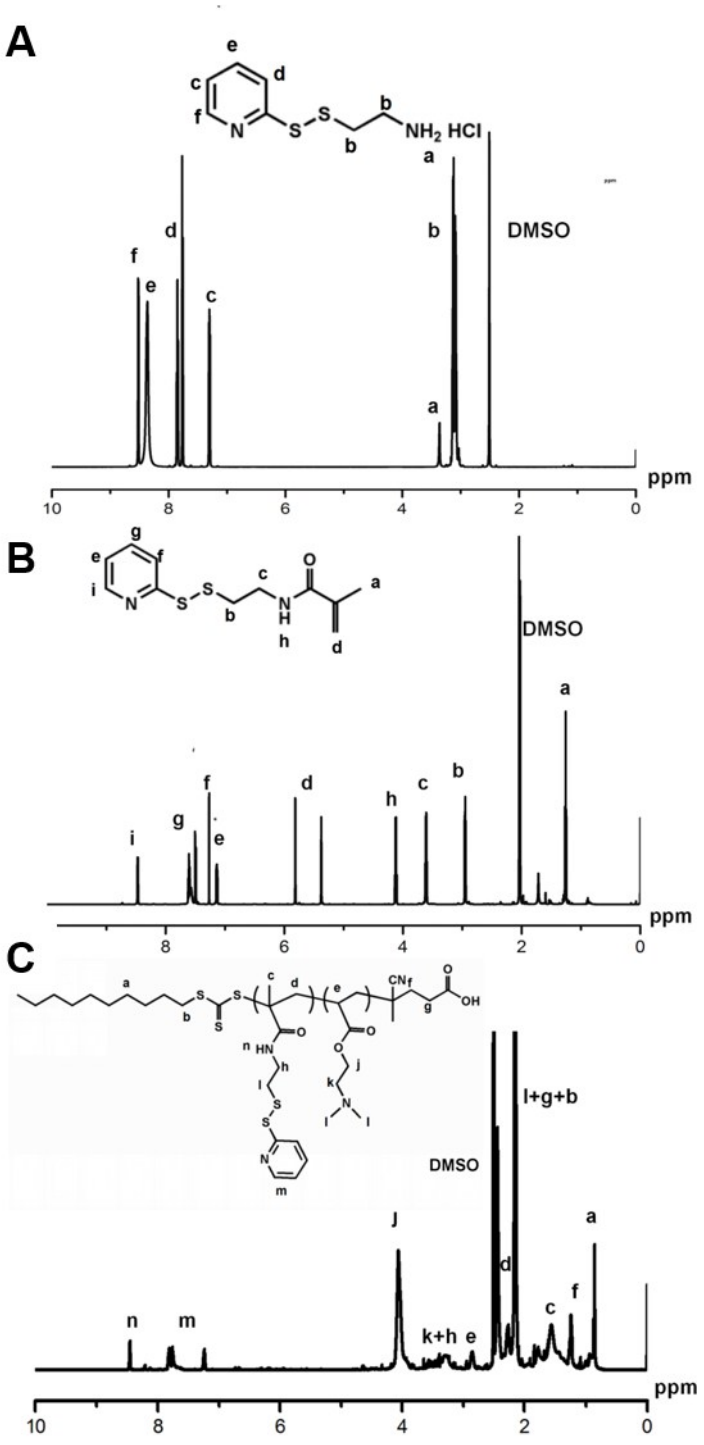

Fig. S4 ^{1}H NMR spectra of DTA (A), PDM (B) and PDM-PDA (C).

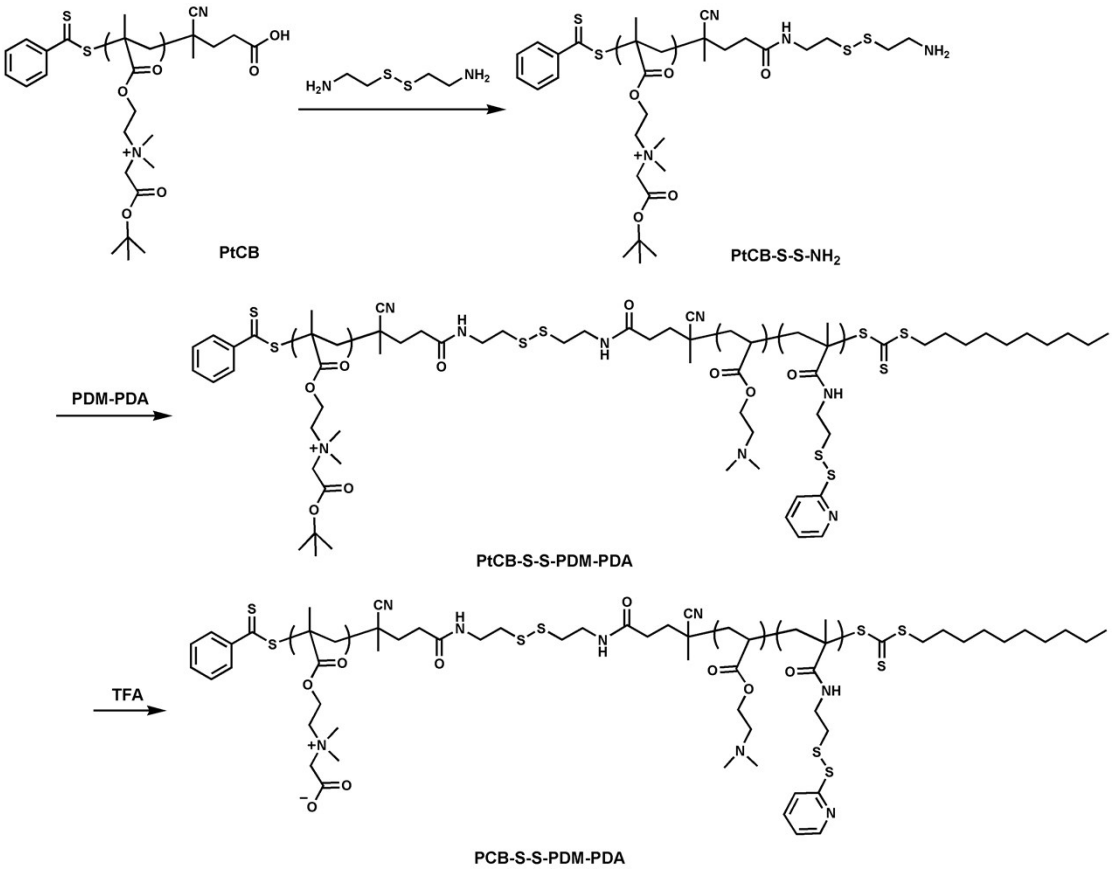

Fig. S5 The synthetic routes of PCB-S-S-PDM-PDA (PSDP).

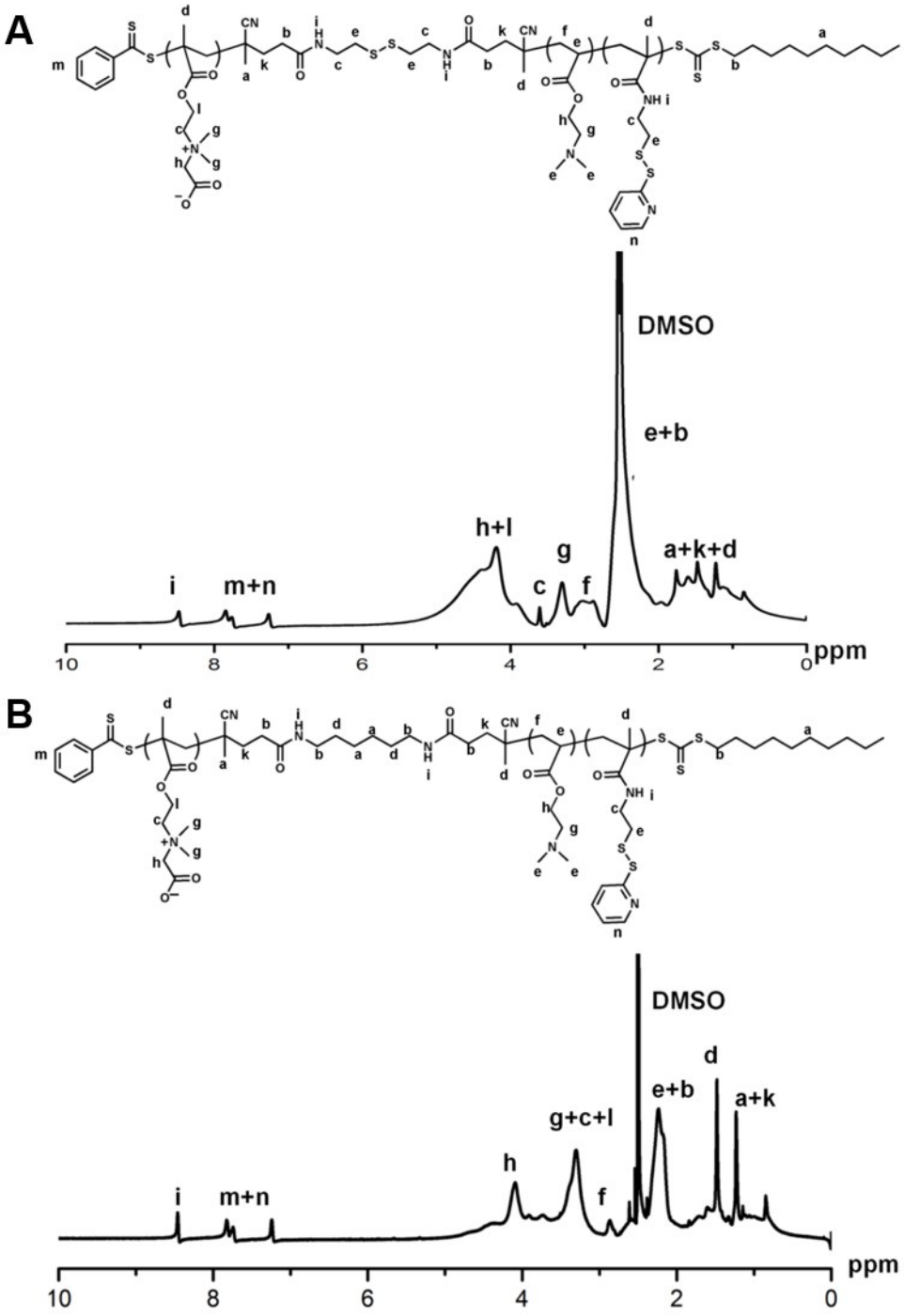

Fig. S6 ^{1}H NMR spectra of PCB-S-S-PDM-PDA (PSDP) (A) and PCB-C-PDM-PDA (PCDP) (B).

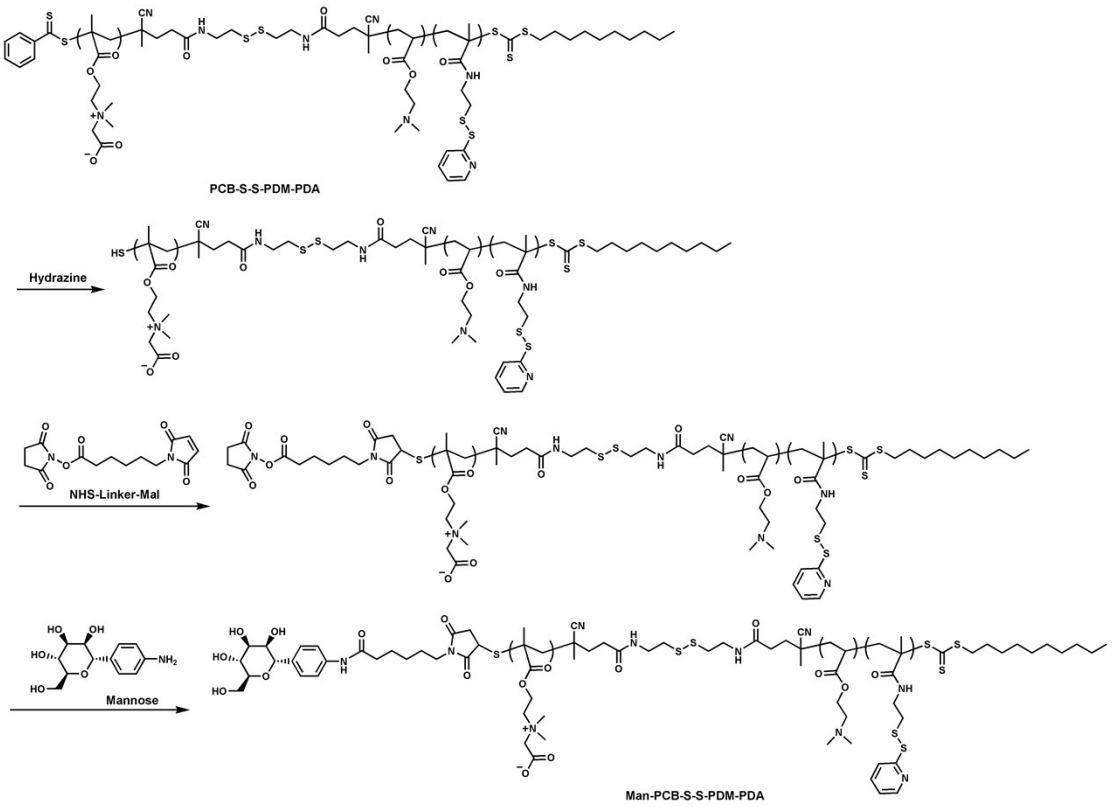

Fig. S7 The synthetic routes of Man-PCB-S-S-PDM-PDA (MPSDP).

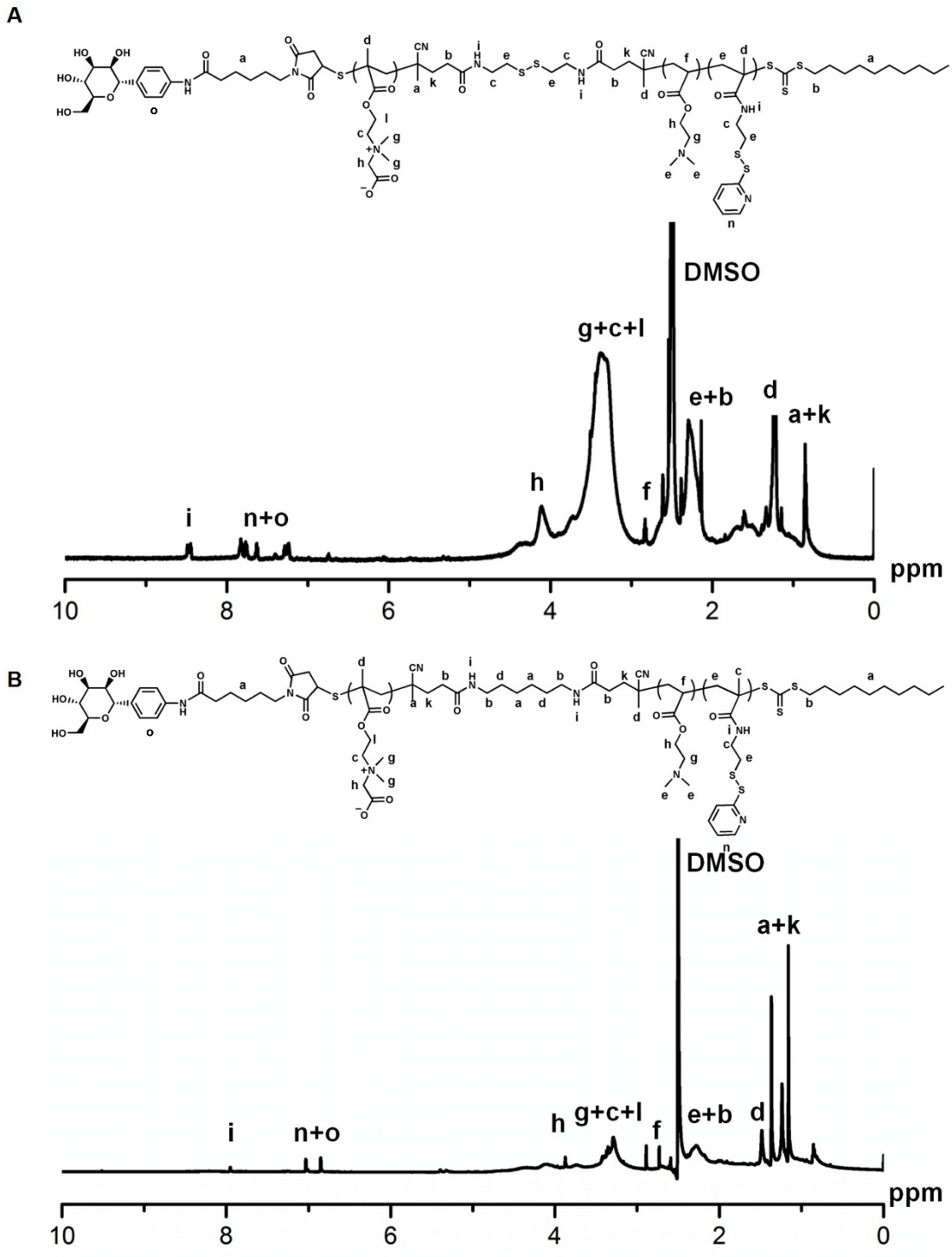

Fig. S8 ^{1}H NMR spectra of Man-PCB-S-S-PDM-PDA (MPSDP) (A) and Man-PCB-C-PDM-PDA (MPCDP) (B).

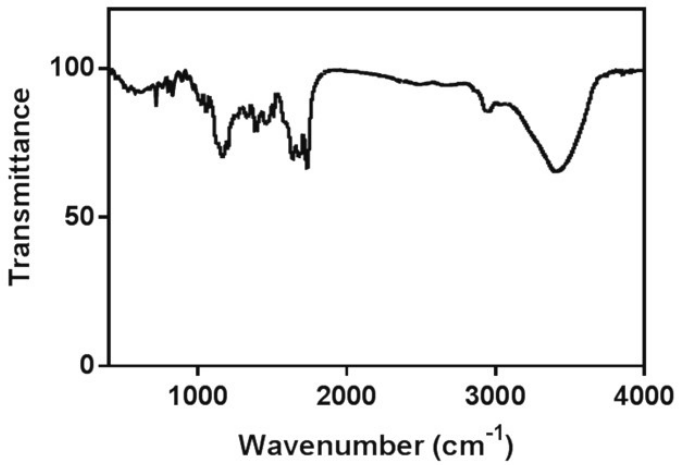

Fig. S9 FTIR spectrum of Man-PCB-S-S-PDM-PDA (MPSDP).

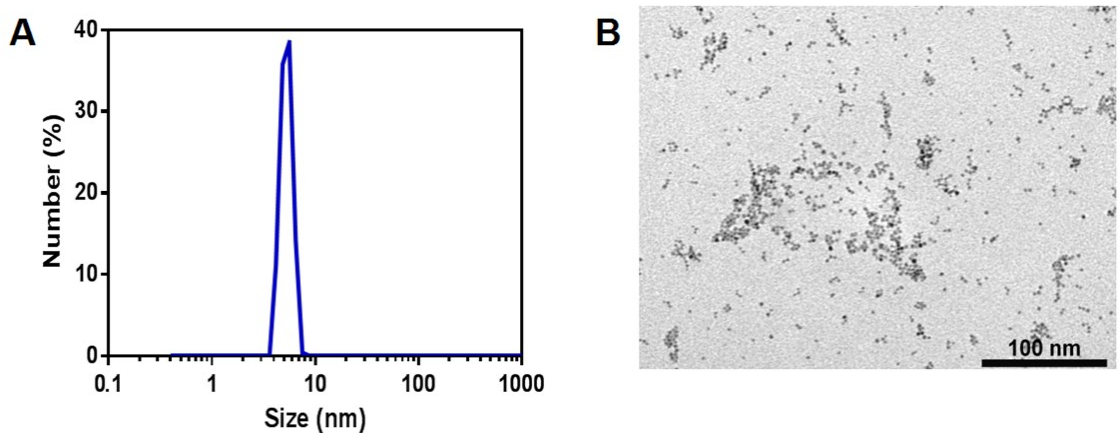

Fig. S10 (A) The size distribution of ZnO NPs. (B) Transmission electron microscopy (TEM) images of ZnO NPs. Scale bar, 100 nm.

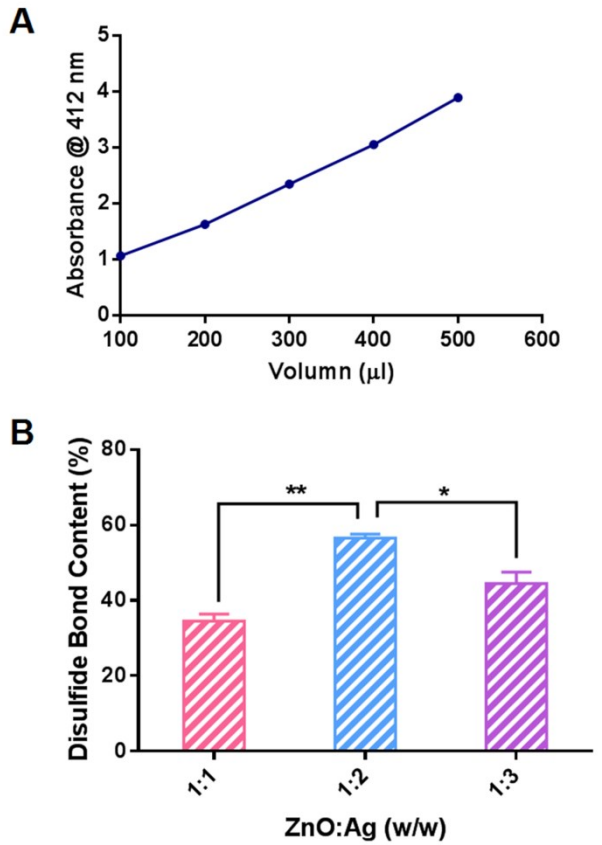

Fig. S11 (A) The absorbance of total thiols in ZnO and Ag solution before reaction. (B) Determination disulfide bond content in different ratio of ZnO/Ag NPs after reaction.

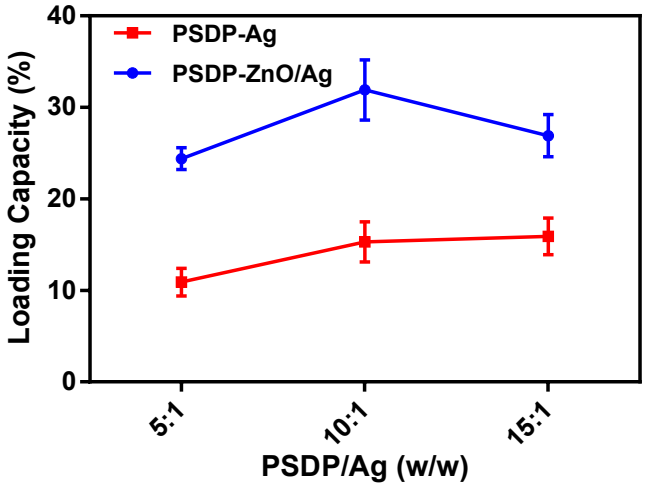

Fig. S12 Loading capacity of PSDP-Ag and PSDP-ZnO/Ag NPs at different ratio of PSDP and Ag.

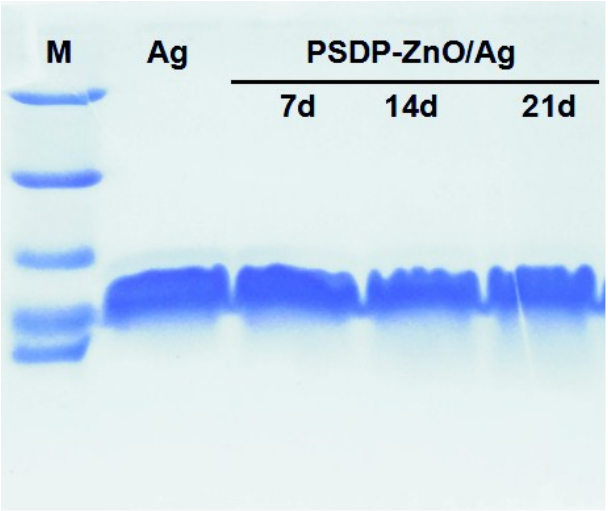

Fig. S13 PSDP-ZnO/Ag NPs offered better protection for antigen stability. The gel electrophoresis of PSDP-ZnO/Ag NPs after 7 d, 14 d and 21 d. Ag was used as a control. M, marker.

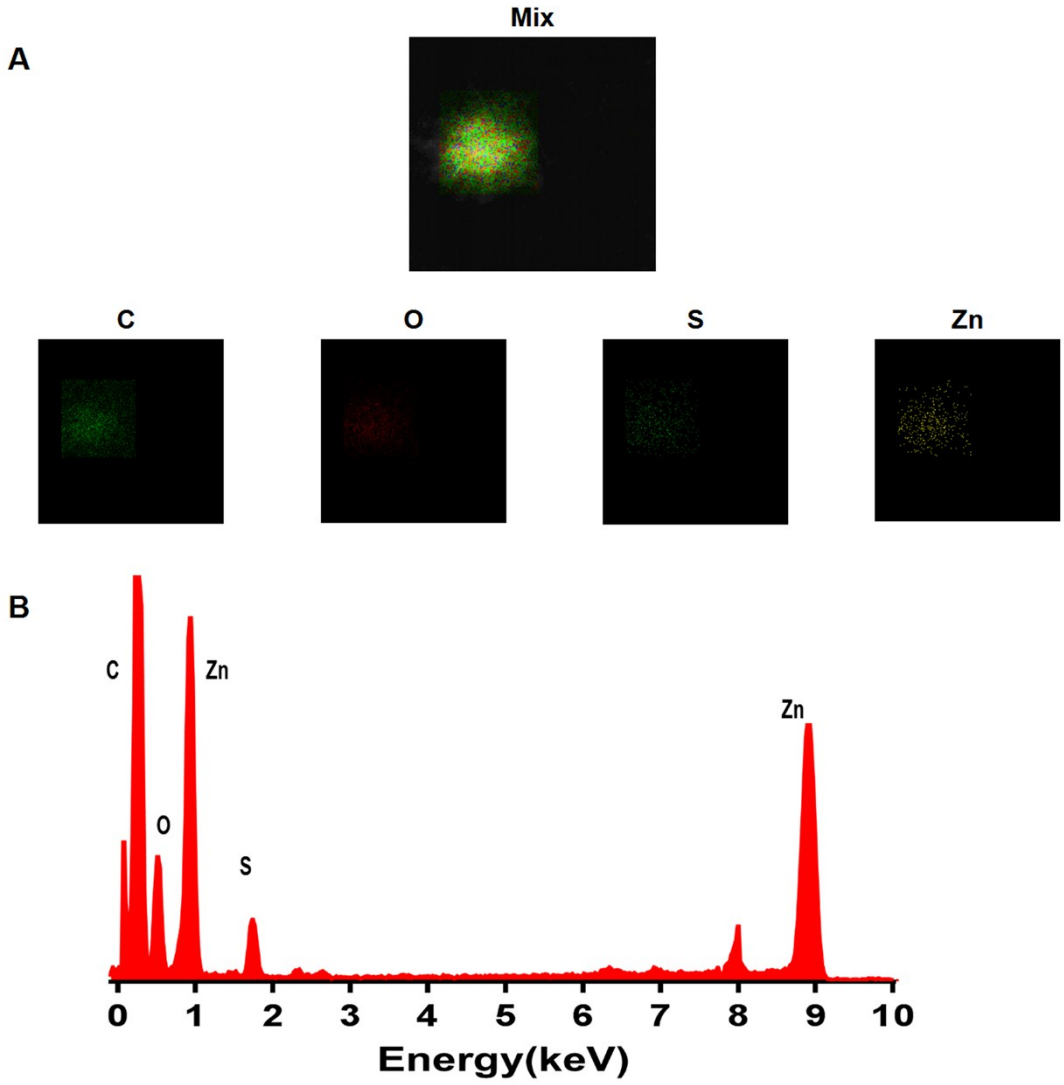

Fig. S14 (A) Elements analysis of PSDP-ZnO/Ag NPs by HRTEM. (B) EDX spectrum of PSDP-ZnO/Ag NPs.

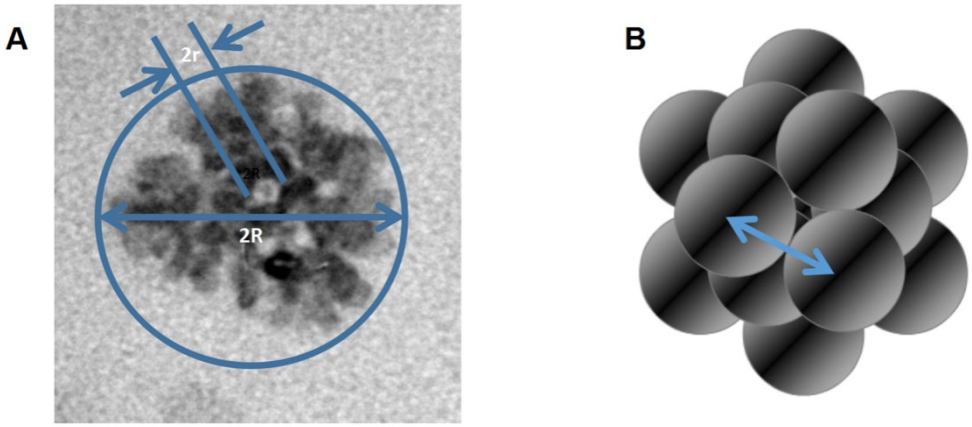

Fig. S15 Geometry estimation on the ZnO NPs loading. (A) The TEM image of PSDP-ZnO/Ag NPs. (B) The schematic diagram of closest packing of the sphere.

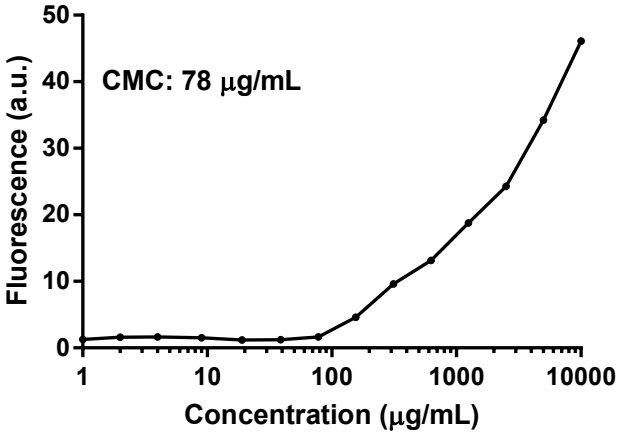

Fig. S16 The fluorescence intensity of nile red as a function of the concentration of PSDP.

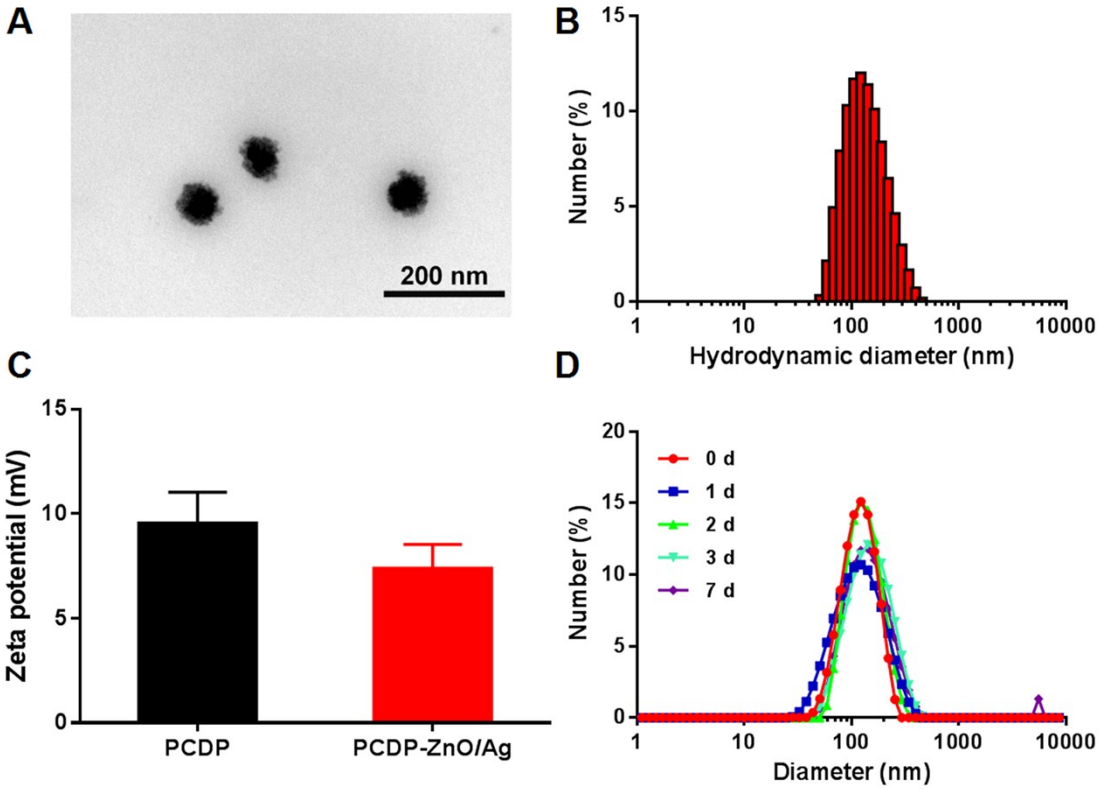

Fig. S17 Characterizations of the non-reductive nanosystems PCDP-ZnO/Ag. (A) The TEM images of PCDP-ZnO/Ag NPs. Scale bar, 200 nm. (B) The size distribution of PCDP-ZnO/Ag NPs in water. (C) The zeta potential of PCDP polymer and PCDP-ZnO/Ag NPs. (D) Size stability of PCDP-ZnO/Ag NPs stored in PBS with 10% serum over 7 d. Date are presented as the mean ± SD.

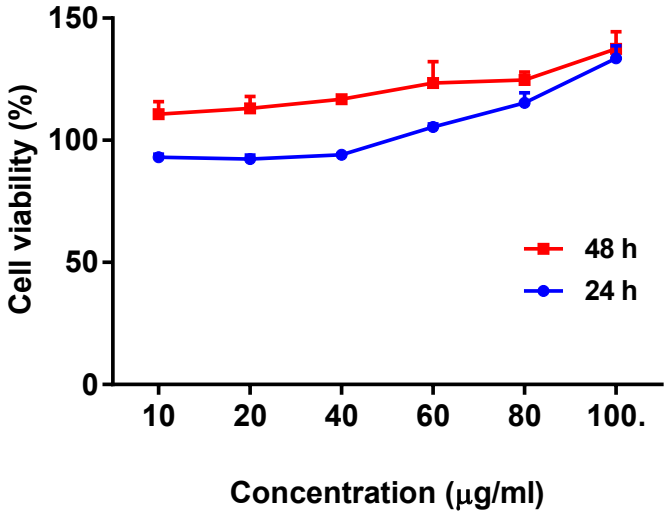

Fig. S18 The cytotoxic effects of nanovaccines on mouse bone marrow derived dendritic cells (BMDCs). BMDCs were cultured with 10-100 μg nanovaccine for 24 h or 48 h at 37°C.

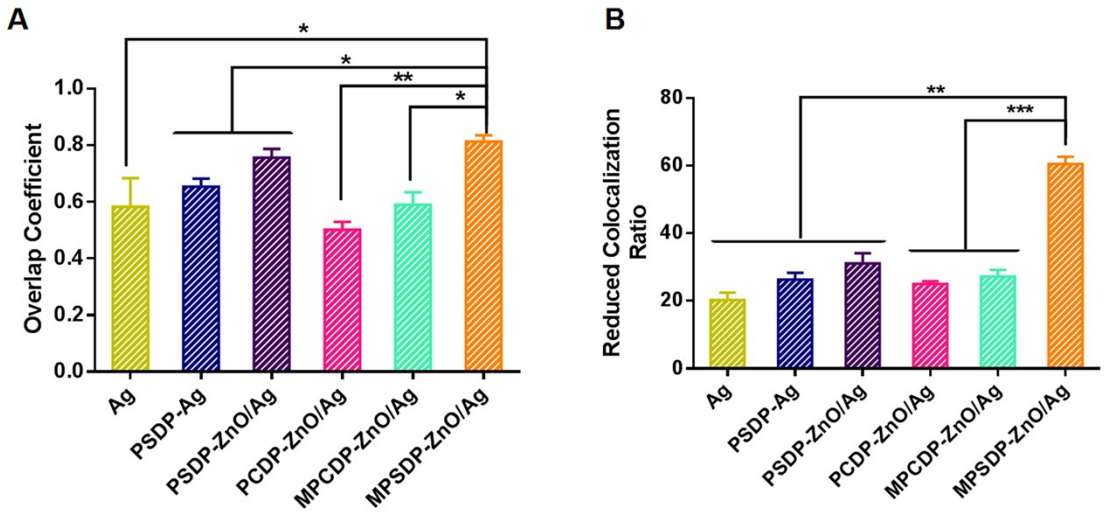

Fig. S19 (A) The overlap coefficients of endosomes/lysosomes and FITC-Ag were calculated by Zen Co-localization software. (B) The reduced co-localization ratio of endosomes/lysosomes and different formulations calculated by the co-localization ratio at 2 h versus the value at 6 h. The co-localization ratios were quantified from Fig. 2C and D by using Zen Co-localization software. Data are presented as the mean ± SD. **: $P < 0.05$, **: $P < 0.01$, ***: $P < 0.001$.

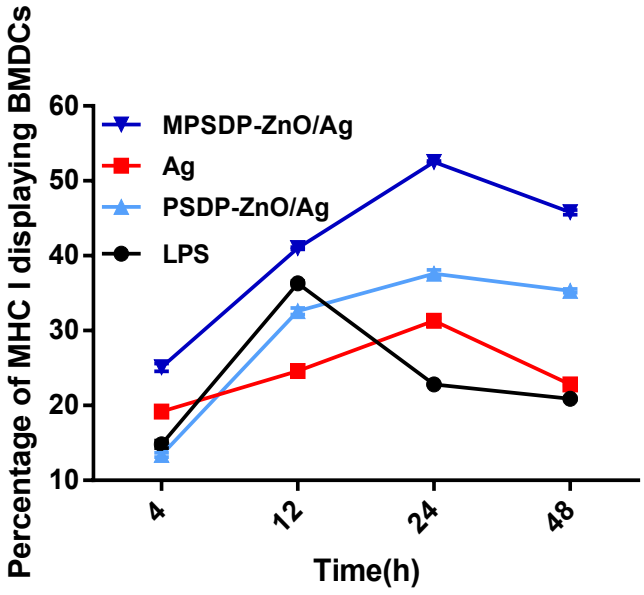

Fig. S20 BMDCs were incubated with nanovaccine formulations for 4 h, 12 h, 24 h, or 48 h, and the antigen presentation was quantified by flow cytometry. The data showed mean ± SD of a representative experiment from 3 independent experiments.

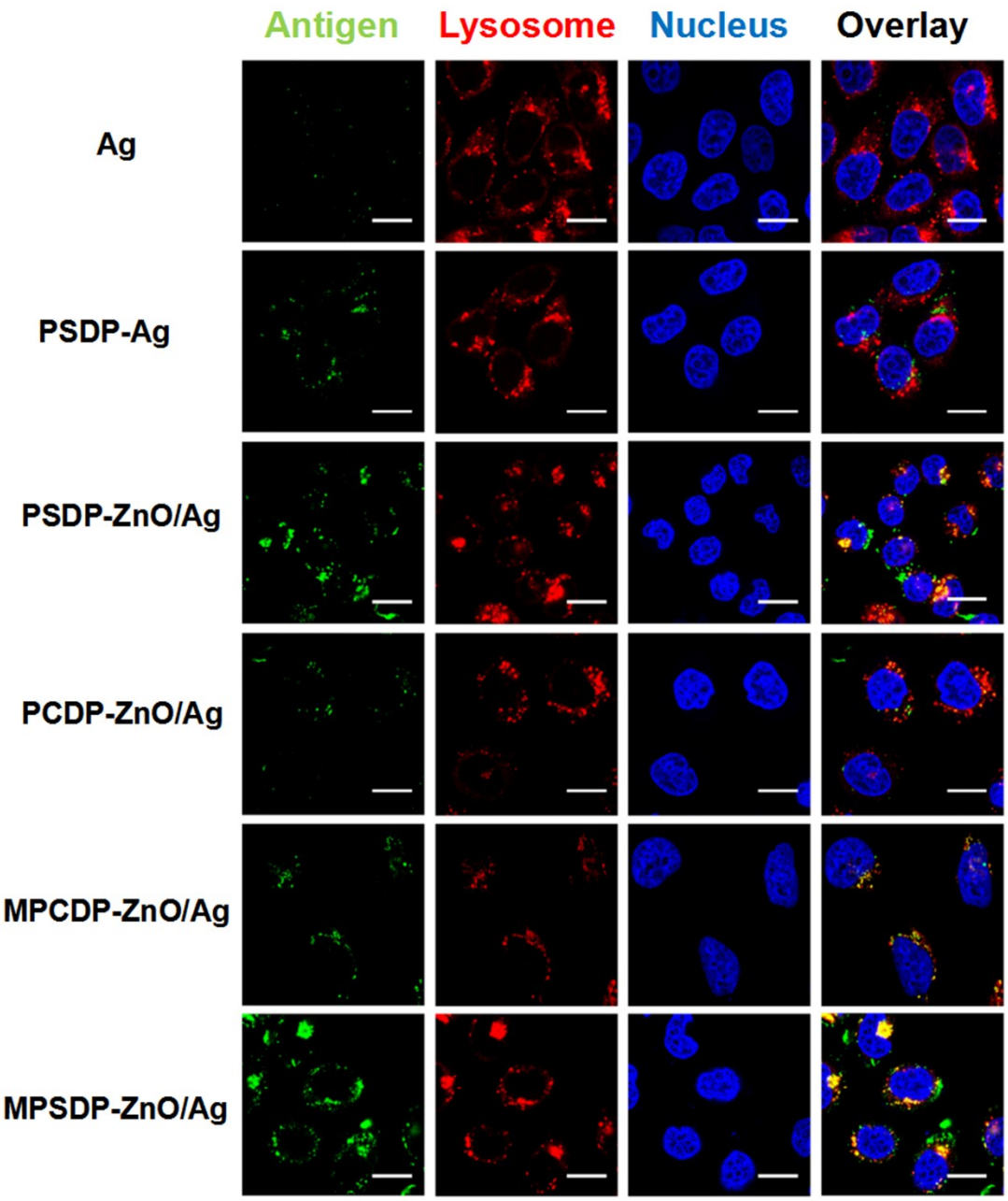

Fig. S21 Delivery and presentation of Ag to immune cells. DC2.4 cells were incubated with Ag, PSDP-Ag, PSDP-ZnO/Ag, PCDP-ZnO/Ag, MPCDP-ZnO/Ag or MPSDP-

ZnO/Ag for 48 h, and then stained with DAPI and Lysotracker Red DND-99. Antigen was labelled by FITC. Scale bar, 20 μm.

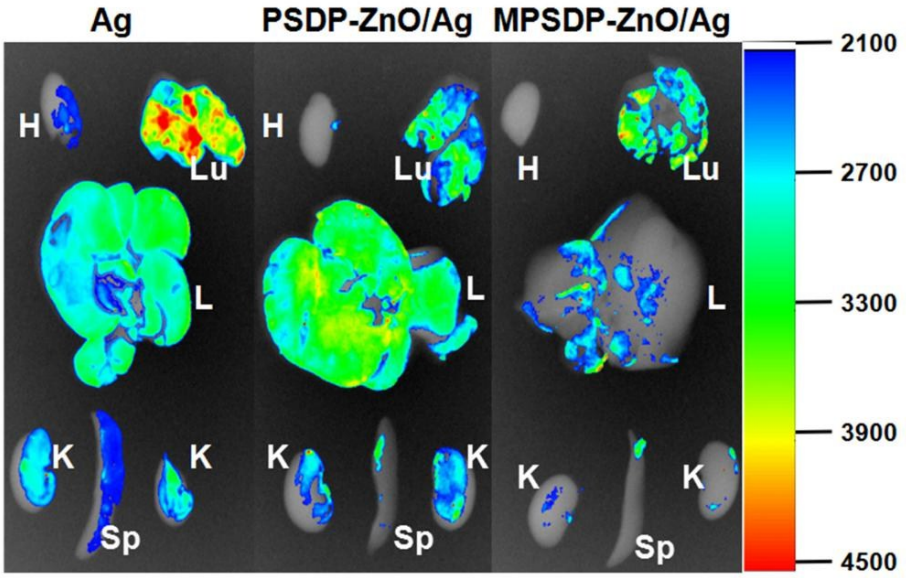

Fig. S22 The accumulation of Ag in normal organs (heart (H), lung (Lu), liver (L), kidney (K) and spleen (Sp)) at 24 h after intravenous injection of different formulations. The equivalent concentration of Ag was 100 μg with FITC as the fluorescence signals.

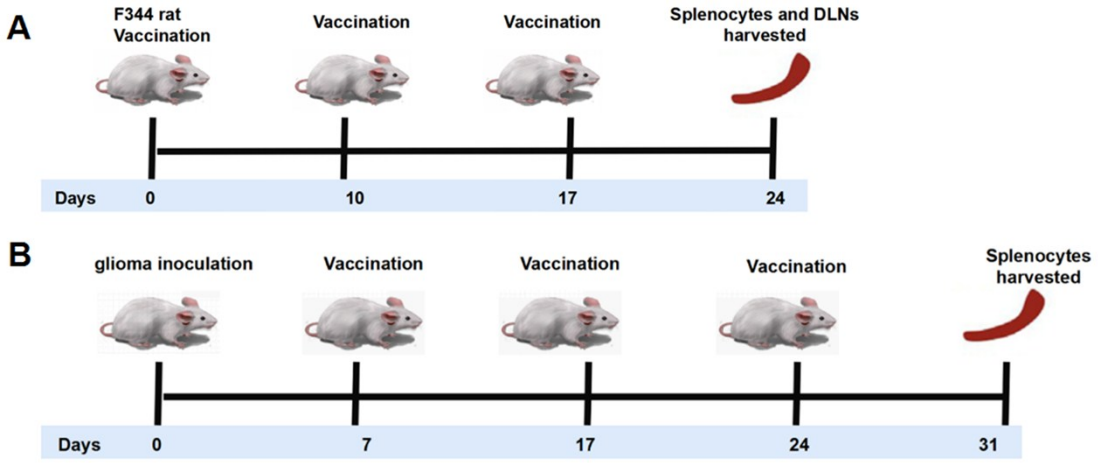

Fig. S23 Female F344 rats (A) and tumor-bearing rats (B) were immunized with nanovaccines for 3 times.

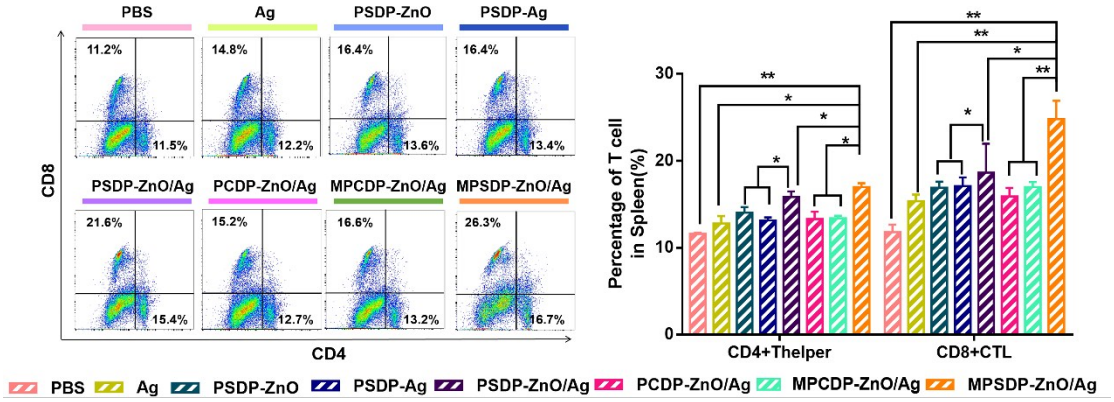

Fig. S24 Female F344 rats were injected intramuscularly with one of the follows: PBS, Ag (100 μg) and different formulations (Ag equivalent content 100 μg). Representative flow cytometry plots of $CD8^+$ cytotoxic T cells and $CD4^+$ T helper cells in spleen were tested for different formulations. The data are shown the mean ± SD, and differences among groups are determined using one-way ANOVA analysis and followed by Tukey's post-test. *p<0.05, **p<0.01, ***p<0.001, and ****p<0.0001.

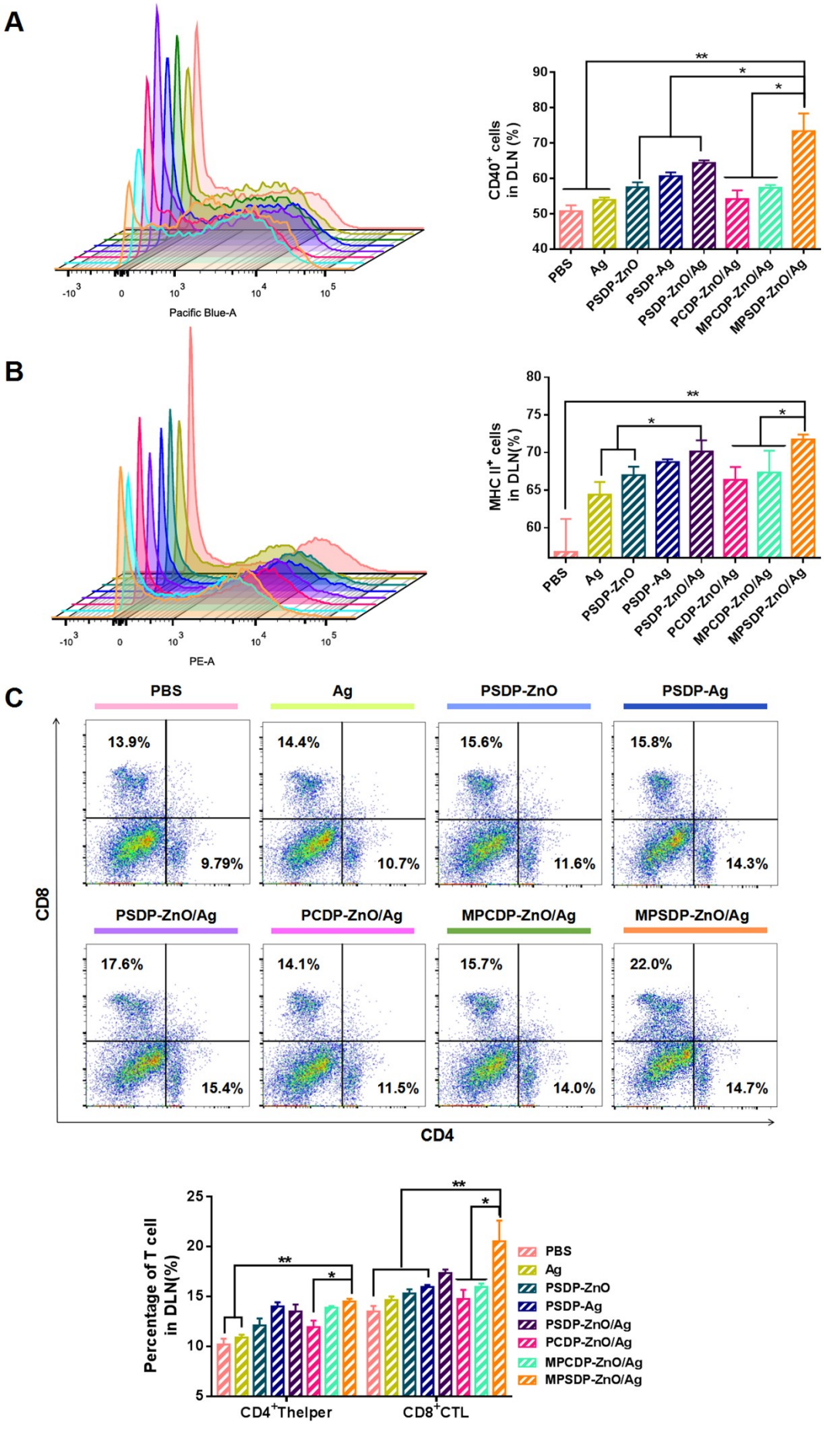
A
Pacific Blue-A
CD40+ cells in DLN (%)
PBS
Ag
PSDP-ZnO
PSDP-Ag
PSDP-ZnO/Ag
PCDP-ZnO/Ag
MPCDP-ZnO/Ag
MPSDP-ZnO/Ag
B
PE-A
MHC II+ cells in DLN(%)
C
PBS
Ag
PSDP-ZnO
PSDP-Ag
13.9%
9.79%
14.4%
10.7%
15.6%
11.6%
15.8%
14.3%
PSDP-ZnO/Ag
PCDP-ZnO/Ag
MPCDP-ZnO/Ag
MPSDP-ZnO/Ag
17.6%
15.4%
14.1%
11.5%
15.7%
14.0%
22.0%
14.7%
CD8
CD4
Percentage of T cell in DLN(%)
CD4+Thelper
CD8+CTL

Fig. S25 Activation of immune responses in draining lymph nodes (DLNs). (A) The expression of $CD40^+$ on the dendritic cells in the DLNs (n = 3). (B) Percentage of major histocompatibility complex class II ($MHC\ II^+$) in DLNs by flow cytometry. (C) Infiltration of immune effector cells in DLNs. Absolute number of $CD4^+$ T helper and $CD8^+$ (CTL) cells in the lymph nodes. The data shown the mean ± SD, and differences among groups are determined by using one-way ANOVA analysis. *p<0.05, **p<0.01.

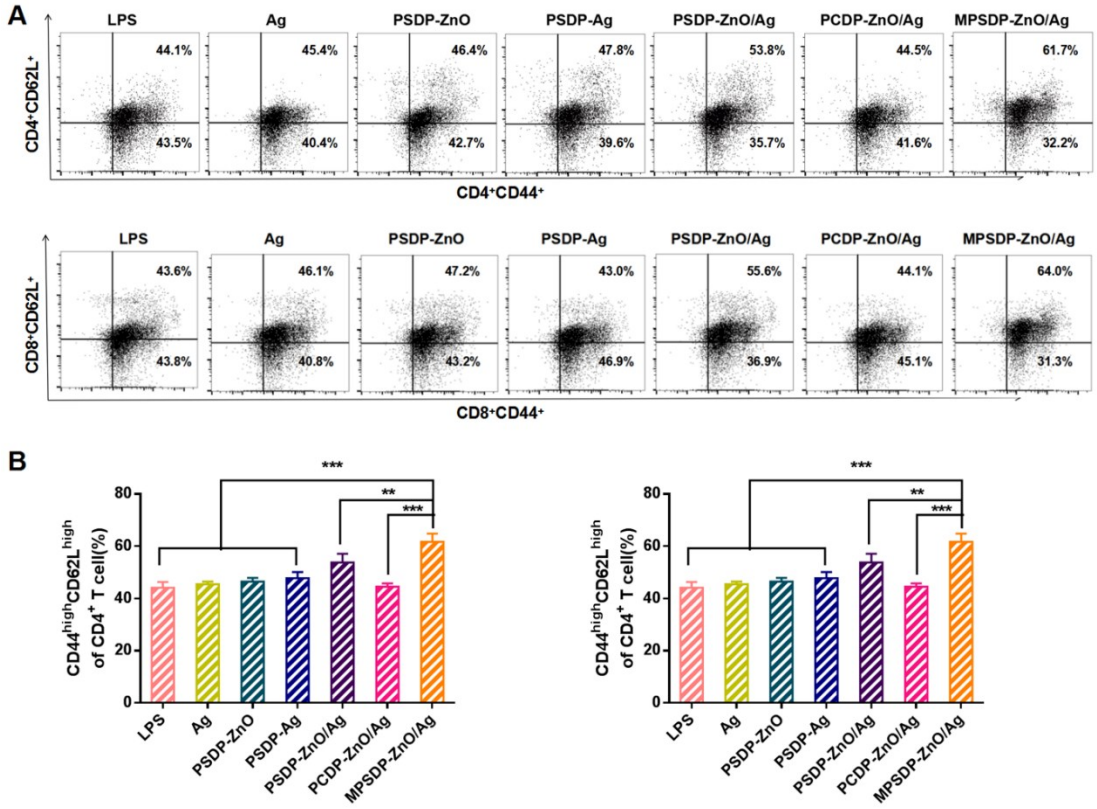

Fig. S26 Proportion of central memory (TCM, $CD44^{Hi}CD62L^{Hi}$) in $CD4^+$ T cells and $CD8^+$ T cells. Tumor-bearing rats were immunized at days 7, 17, 24. Splenocytes were collected and stained with fluorescent-labeled antibody. The proportion of the $CD44^{Hi}CD62L^{Hi}/CD4^+$ T-cell, $CD44^{Hi}CD62L^{Hi}/CD8^+$ T-cell were determined by flow

cytometry. Representative FACS plots are shown (A). Data (B) are expressed as mean ± SD was shown (n=3). **: P < 0.01, ***: P < 0.001.

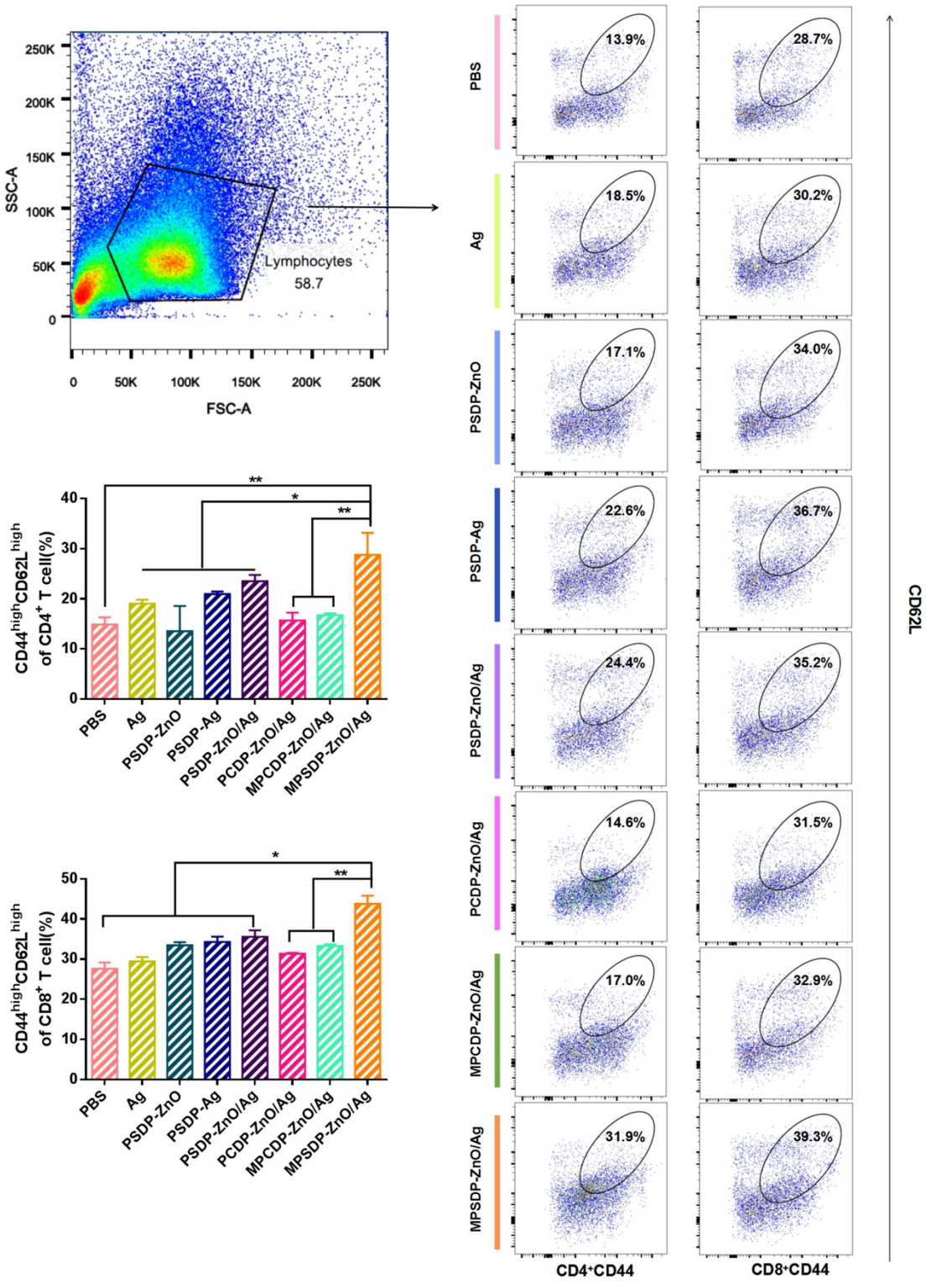

Fig. S27 Proportion of central memory (TCM, $CD44^{Hi}CD62L^{Hi}$) in $CD4^+$ T cells and

$CD8^+$ T cells. The normal F344 rats were immunized at days 0, 10, 17. Splenocytes were collected and stained with fluorescent-labeled antibody. The proportion of the $CD44^{Hi}CD62L^{Hi}/CD4^+$ T-cell, $CD44^{Hi}CD62L^{Hi}/CD8^+$ T-cell were determined by flow cytometry (A). Data (B) are expressed as mean ± SD (n=3). *p<0.05, **: P < 0.01.

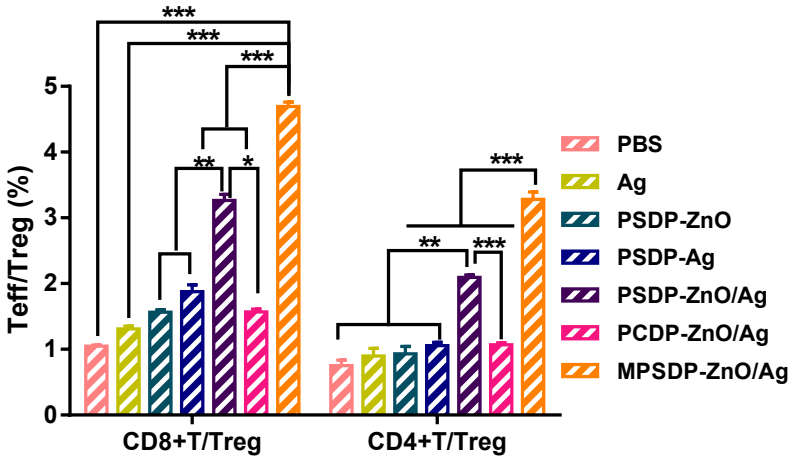

Fig. S28 The percentage of Teff/Treg in spleen upon various treatments in tumor-bearing rats were quantified by flow cytometric analysis. Data are presented as the mean ± SD. *p<0.05, **p<0.01, ***p<0.001, and ****p<0.0001.

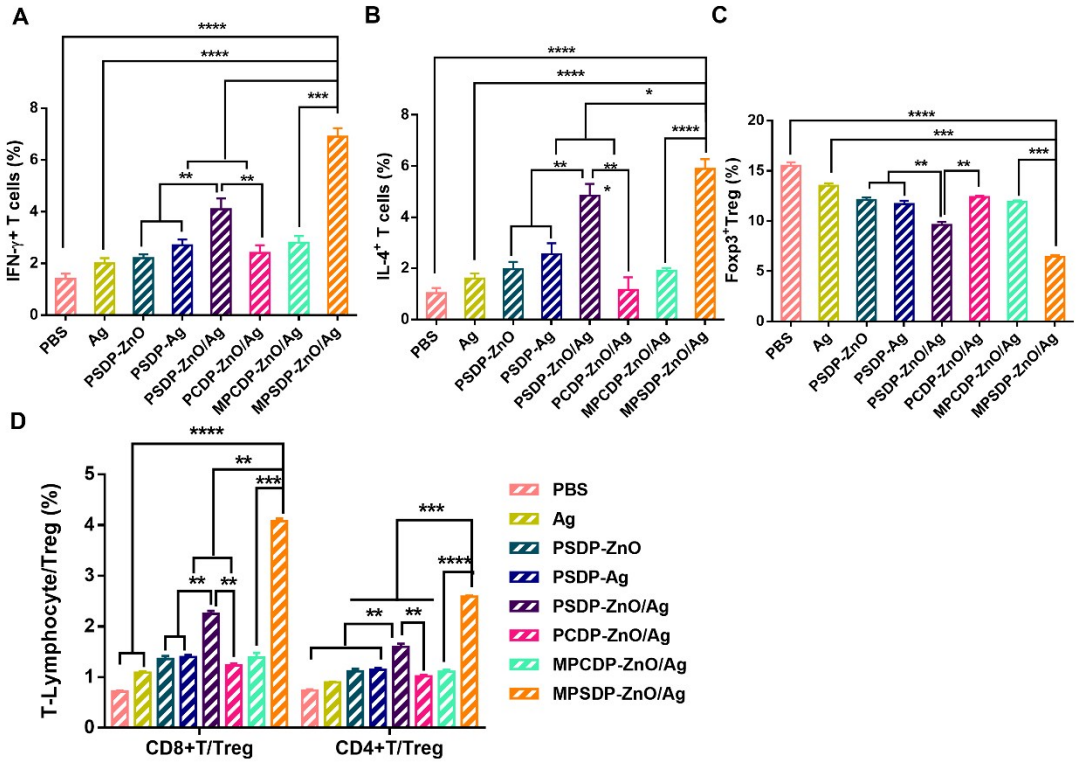

Fig. S29 F344 rats were immunized with various formulations for 3 times. The proportion of IFN-γ (A), IL-4 (B) and Foxp3 (C) in $CD4^+$ T cells on day 24 in spleen from rats vaccinated by flow-cytometry analysis. (D) The frequency of $CD8^+$ T/Treg and $CD4^+$ T/Treg in spleen upon various treatments were quantified by flow cytometric analysis. Data are presented as the mean ± SD. $^*p<0.05$, $^{**}p<0.01$, $^{***}p<0.001$, and $^{****}p<0.0001$.

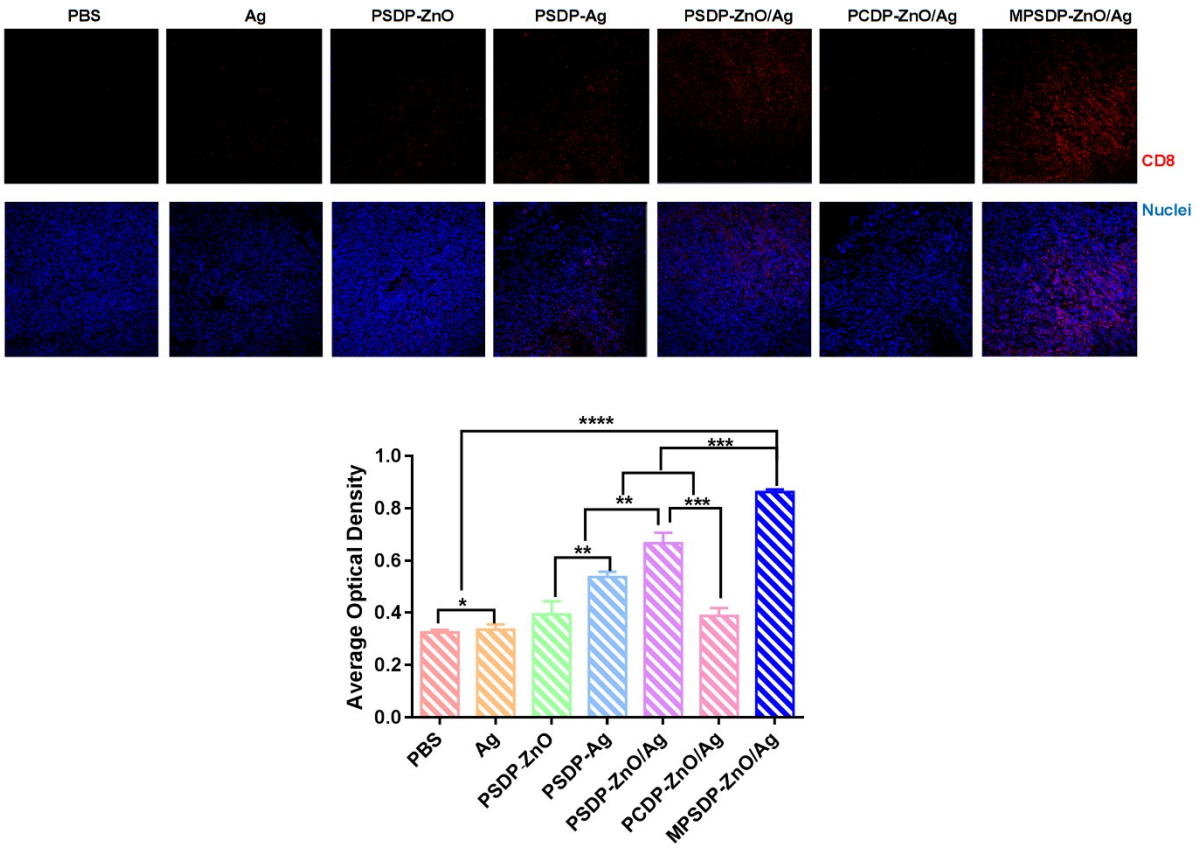

Fig. S30 The effect of cancer vaccines on $CD8^+$ T cells in tumor bearing rats. F344 tumor bearing rats were intramuscular injected with different vaccines on day 7, 17, 24 post tumor inoculation. 7 days after 3 rd injection, tumor was dissected and then snap frozen. Brain tumor tissues were labelled with immunofluorescence antibody, and immunofluorescence images were recorded by using a confocal microscopy. Bars are shown as mean ± SD, and the differences among groups are analyzed by using one-way

ANOVA analysis and followed by Tukey's post test. *: $p < 0.05$, **: $p < 0.01$, ***: $p < 0.001$, ****: $p < 0.0001$.

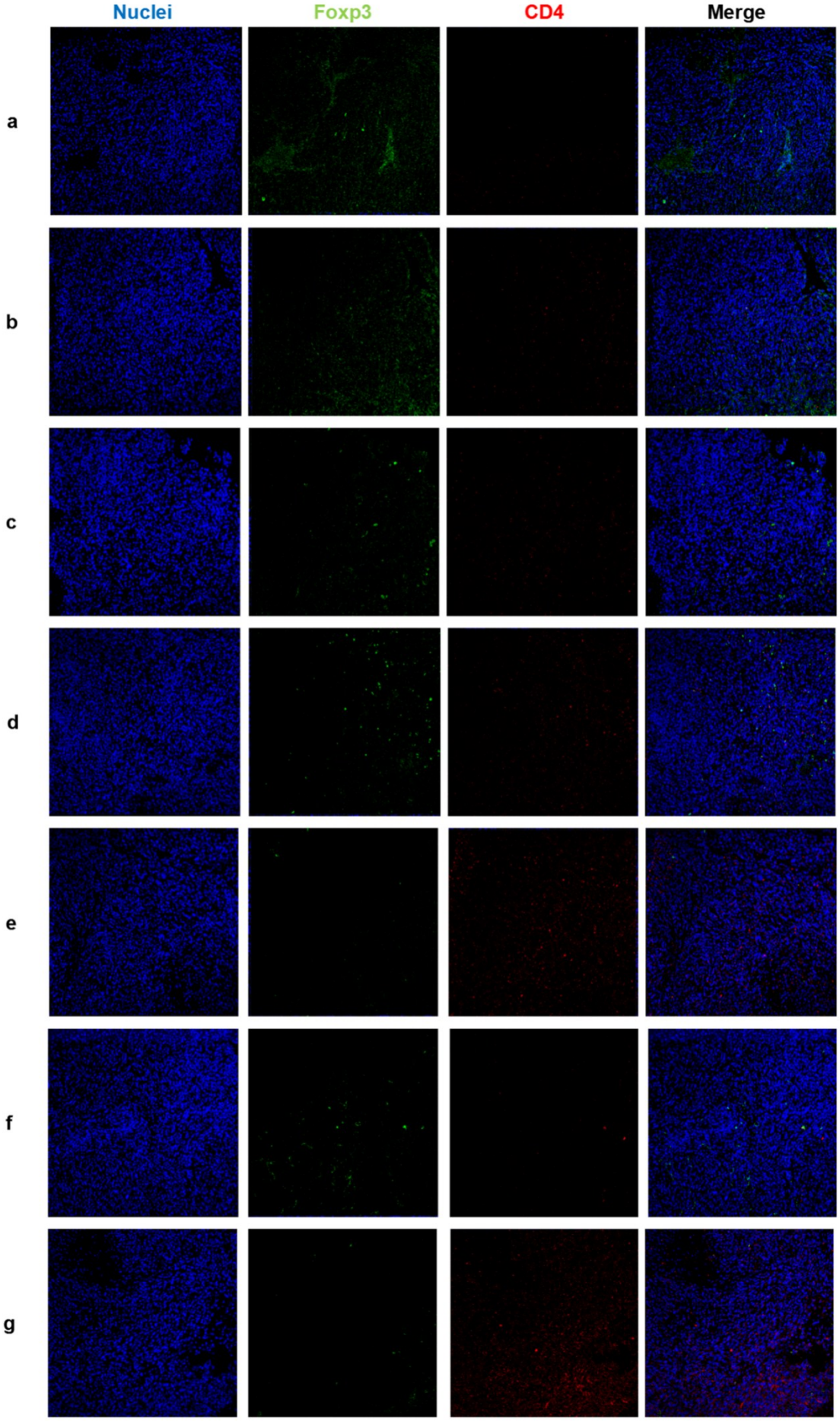
Nuclei
Foxp3
CD4
Merge
a
b
c
d
e
f
g

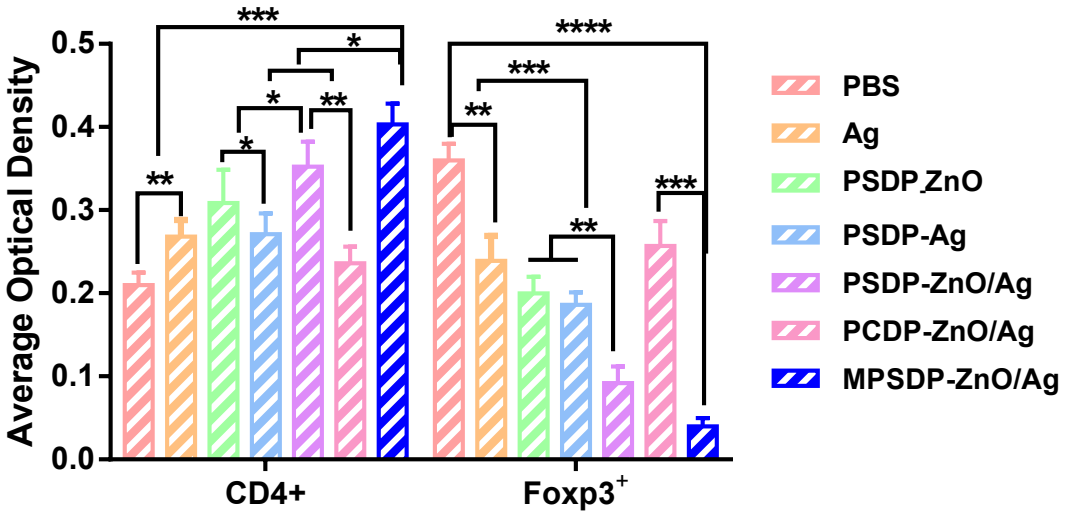

Fig. S31 The immunofluorescence results of $CD4^+$ and $Foxp3^+$ T cells of glioma-bearing mice treated with different formulations, including (a, PBS; b, Ag; c, PSDP-ZnO; d, PSDP-Ag; e, PSDP-ZnO/Ag; f, PCDP-ZnO/Ag; g, MPSDP-ZnO/Ag). *: $P < 0.05$, **: $P < 0.01$, ***: $P < 0.001$, ****: $P < 0.0001$.

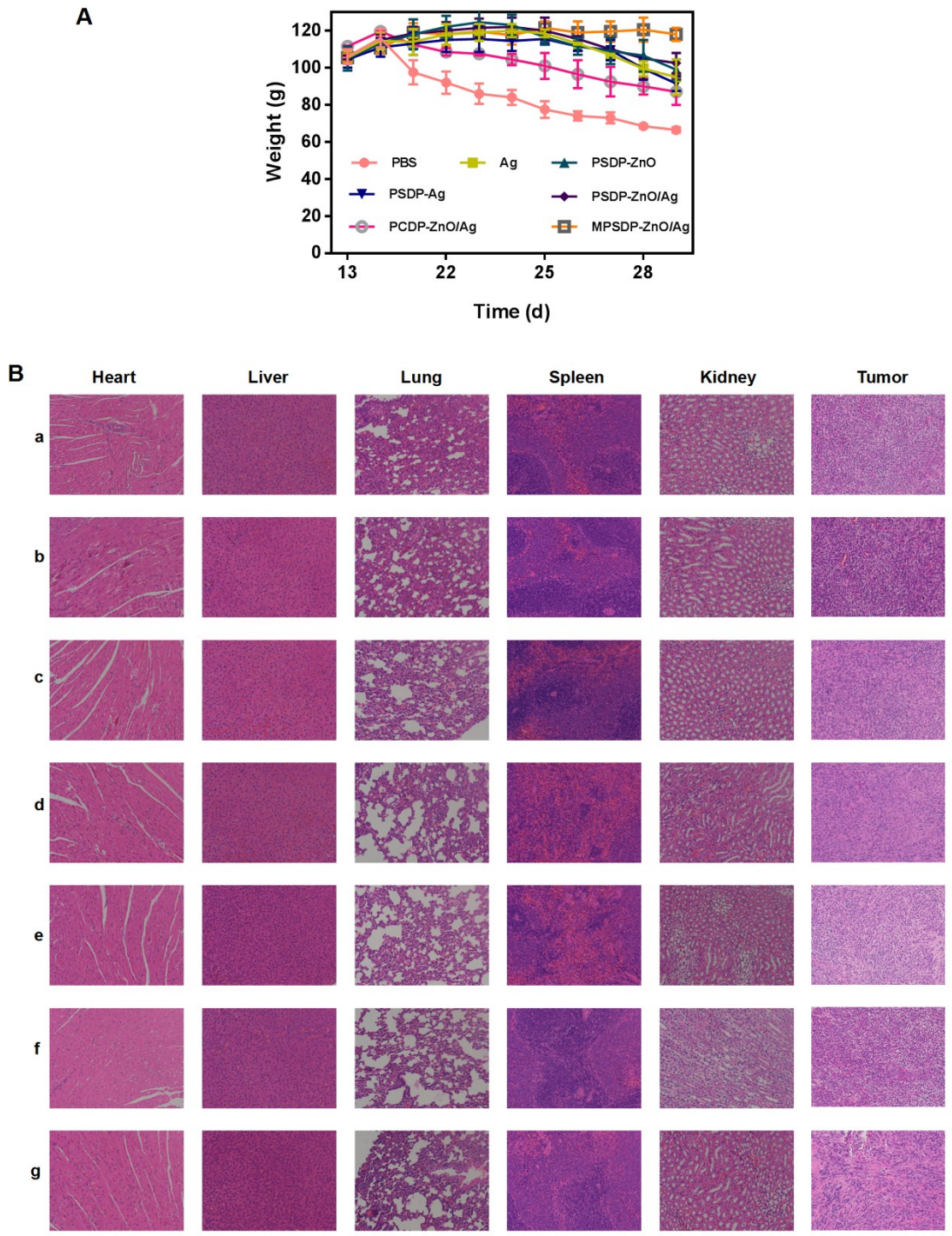

Fig. S32 (A) Time course of F98$_{npEGFRvIII}$-bearing rat weight were measured. (B) Representative H&E staining images of major normal organs and tumors from the treated rats (a, PBS; b, Ag; c, PSDP-ZnO; d, PSDP-Ag; e, PSDP-ZnO/Ag; f, PCDP-ZnO/Ag; g, MPSDP-ZnO/Ag). Magnification: 200×. All data are expressed as mean ± SD.

Note S1 Geometric calculation of PSDP-ZnO/Ag NPs

As shown in Fig. S15, the number of small particles on spherical was predicted under the following assumptions:

(1) small nanoparticles could be seen as spherical particles of radius, r

(2) the spherical particles are same radius of spherical

(3) PSDP-ZnO/Ag nanoparticles could be seen as close-packing of equal the spherical particles.

(4) r, radius of the spherical particles was calculated from measuring the distance of the closest two the spherical nanoparticles on surface of same radius of spherical in Figure S15a:

$2\ r = 13.4 \pm 0.3$ nm

(5) R, radius of PSDP-ZnO/Ag nanoparticle was measured from Figure S15a:

$2\ R = 110 \pm 0.5$ nm

Under the above assumptions,the number of small particles on spherical was calculated from the volume of PSDP-ZnO/Ag nanoparticle.

In geometry, close-packing of equal spheres is a dense arrangement of congruent spheres in an infinite, regular arrangement (or lattice). Carl Friedrich Gauss proved that the highest average density – that is, the greatest fraction of space occupied by spheres – that can be achieved by a lattice packing is $\frac{\pi}{3\sqrt{2}} \approx 0.74$

The volume of the spherical particles of radius, r:

$$V_{\mathrm{r}} = \frac{4\pi}{3} r^3 = \frac{4\pi}{3} \times (\frac{13.4}{2})^3 = 1259 nm^3$$

The volume of the spherical PSDP-ZnO/Ag nanoparticle of radius, R:

$$V_{\mathrm{R}} = \frac{4\pi}{3} \mathrm{R}^3 = \frac{4\pi}{3} \times (\frac{110}{2})^3 = 696556 nm^3$$

The number of small particles on spherical:

$$N = \frac{V_R \times 0.74}{V_r} = \frac{696556 \times 0.74}{1259} = 410$$